MODULATION OF FGF1 SIGNALING REDUCES PROFIBROTIC, PROLIFERATIVE, AND INFLAMMATORY PHENOTYPES IN THE MDR2$^{-/-}$ MOUSE MODEL OF CHOLESTASIS

A Dissertation

by

APRIL O'BRIEN

Submitted to the Graduate and Professional School of
Texas A&M University
in partial fulfillment of the requirements for the degree of

DOCTOR OF PHILOSOPHY

Chair of Committee,	Shannon Glaser
Committee Members,	Cynthia Meininger
	Chaodong Wu
	Sanjukta Chakraborty
Head of Department,	Carol Vargas

December 2021

Major Subject: Medical Sciences

ABSTRACT

Cholangiopathies, such as primary sclerosing cholangitis (PSC), are progressive liver diseases that target the cholangiocyte and are characterized by inflammation, proliferation, fibrosis, and senescence, for which only limited treatment options are available. Studies have shown microRNA 16 (miR-16) plays a prominent role in profibrotic liver diseases in addition to fibroblast growth factor 1 (FGF1), which contributes to hepatic fibrosis through the activation of hepatic stellate cells (HSCs). However, the role of miR-16 in conjunction with FGF1 in the progression of cholangiopathies such as PSC, is unknown. Therefore, the goal of this study was to evaluate the role of FGF1 in the progression of biliary damage and assess its correlation with miR-16 in mouse models of liver pathology. Male multi-drug resistant 2 ($Mdr2^{-/-}$) or bile-duct ligated (BDL) C57BL/6 mice (12 weeks old) and corresponding controls were treated with either an FGF1 agonist, FGF receptor antagonist (AZD4547), or FGF1 monoclonal antibody ($Mdr2^{-/-}$ and control). We measured: (i) FGF1, FGF receptors (FGFR), miR-16, and angiogenesis via immunofluorescence (IF), quantitative polymerase chain reaction (*q*PCR), or enzyme-linked immunosorbent assay in liver sections, isolated cholangiocytes, and serum; (ii) biliary proliferation by immunohistochemistry (IHC) for cytokeratin-19 and *q*PCR for proliferation genetic markers *Ki67* and proliferating cell nuclear antigen (*PCNA*) in isolated cholangiocytes; (iii) inflammatory markers by *q*PCR and IHC in total liver homogenates and liver sections; (iv) biliary senescence via senescence associated β galactosidase, IF, and *q*PCR;

and (v) fibrosis using Sirius Red and *q*PCR for collagen type 1 alpha 1 (*Col1α1*) and alpha smooth muscle actin (*αSMA*). *In vitro,* we treated cholangiocytes and HSCs with FGF1 monoclonal antibody and measured genes of proliferation/senescence. We found significant increases in FGF1/FGFR expression, biliary proliferation, angiogenesis, liver inflammation, and fibrosis in $Mdr2^{-/-}$ mice with corresponding decreases in miR-16. However, $Mdr2^{-/-}$ mice treated with either an FGFR antagonist or anti-FGF1 mAb displayed a significant reduction in liver fibrosis, senescence, inflammation, angiogenesis, and biliary proliferation. We have demonstrated that disruption of FGF1/FGFR signaling ameliorates fibrosis, proliferation, senescence, angiogenesis, and inflammation in a mouse model of cholestasis, and disruption or activation of the FGF1/FGFR pathway correlates with increased/decreased miR-16 gene expression. In conclusion, the FGF1/FGFR signaling pathway may provide novel therapeutic targets in the fight against PSC.

DEDICATION

This dissertation is dedicated to all the people who believed I could and supported me along this journey. From my oldest children, who were there from the very beginning as I started college and then graduate school, to my Littles, who don't know anything other than my life in graduate school. From my mom, who always believed in me and helped where she could along the way, to my husband, my best friend, and my biggest supporter. For the endless meals you cooked, the laundry you did, and the numerous times you had to take on all the parenting duties, I am so grateful and blessed to have you with me these last five and a half years; I could not have done this without you by my side.

ACKNOWLEDGMENTS

First and foremost, I would like to thank my committee chair, Dr. Shannon Glaser, for not only her support as an employer and mentor but also for being a strong role model who demonstrates you can be both a mom and a scientist with success. I also would like to extend a heartfelt thanks to my committee members, Dr. Meininger, who was a part of my committee through our lab moving twice and the inhabitation of 3 different locations, and Drs. Wu and Chakraborty who kindly agreed to join my committee when we finally settled in College Station. Finally, I would like to thank my lab members who have come and sometimes moved on; I learned something from each of you during this process.

CONTRIBUTORS AND FUNDING SOURCES

Contributors

This work was conducted under the supervision of a dissertation committee headed by Dr. Shannon Glaser, Drs. Cynthia Meininger and Sanjukta Chakraborty in the Department of Medical Physiology, and Dr. Chaodong Wu in the Department of Nutrition and Food Science.

This dissertation contains research that was submitted to *Hepatology Communications* by April O'Brien and coauthors.

Additional work for this dissertation was completed by the student independently.

Funding Sources

This work was supported by the Hickam Endowed Chair, Gastroenterology, Medicine and the Research Career Scientist award from the United States Department of Veteran's Affairs, Biomedical Laboratory Research and Development Service (to Gianfranco Alpini [GA]), Indiana University; the Indiana University Health – Indiana University School of Medicine Strategic Research Initiative (GA and Heather Francis [HF]); NIH grants DK108959 and DK119421 (HF), DK054811, DK115184, DK076898, DK110035, DK062975 (GA and Shannon Glaser [SG]), and partially by funds from the Baylor Scott & White Research Institute. Material supported was provided by the Central Texas Veterans Health Care System, Temple, TX, and the Richard L. Roudebush VA

Medical Center, Indianapolis, IN. The content and views are those of the authors and do not necessarily represent the views or policies of the Department of Veterans Affairs or the United States Government.

NOMENCLATURE

α-SMA	alpha smooth muscle actin
abcb4	ATP binding cassette subfamily B member 4
ANG	angiogenin
BDL	bile duct ligation
CCA	cholangiocarcinoma
CCl_4	carbon tetrachloride
CD31	platelet cell adhesion molecule 1
CK-19	cytokeratin-19
Col1a1	collagen, type I, alpha 1
DAPI	4’,6-diamidino-2-phenylindole
DDC	dihydrocollidine
ECM	extracellular matrix
ELISA	enzyme-linked immunosorbent assay
FFPE	formalin fixed paraffin embedded
FGF	fibroblast growth factor
FGFR	fibroblast growth factor receptor
Fn1	fibronectin 1
GAPDH	glyceraldehyde-3-phosphate dehydrogenase

H69	human cholangiocyte cell line
HGF	hepatocyte growth factor
HSCs	human hepatic stellate cells
IBDM	intrahepatic bile duct mass
IL	interleukin
IPA	ingenuity pathway analysis
Ki67	cell proliferation antigen Ki67
LCA	lithocholic acid
$Mdr2^{-/-}$	multidrug resistant gene 2 knockout
miR-16	microRNA 16
p16	cyclin-dependent kinase inhibitor 2A
p21	cyclin-dependent kinase inhibitor 1A
p53	tumor protein 53
PBC	primary biliary cholangitis
PCNA	proliferating cell nuclear antigen
PCR	polymerase chain reaction
PSC	primary sclerosing cholangitis
rhFGF1	recombinant human FGF1
ROS	reactive oxygen species

SA-β-gal	senescence associated β galactosidase
TGF-β1	transforming growth factor-beta 1
VEGFA	vascular endothelial growth factor A
WT	wild type

TABLE OF CONTENTS

Page

LIST OF FIGURES

Page

LIST OF TABLES

Page

CHAPTER I

INTRODUCTION AND LITERATURE REVIEW

Cholangiopathies

Cholangiopathies are a group of chronic liver diseases that target the cholangiocyte, a small heterogeneous subset of cells that line the biliary tree and function in bile modification, liver repair, and interactions with the hepatic environment through exogenous and endogenous communications.[1] Cholangiopathies affect all ages, from infancy in the form of biliary atresia, to cholangiocarcinoma, where the average age of patients is 65 years or older at the time of diagnosis. Six main cholangiopathies share several characteristics, including a pro-inflammatory response, proliferation and differentiation, tissue repair, fibrosis, and bile flow impediment.[1-3] Due to the invasive, aggressive, varying nature of cholangiopathies, relatively few treatment options are available. The resultant end-stage liver failure often culminates in costly yet dangerous liver transplantation.

Primary Sclerosing Cholangitis

Primary sclerosing cholangitis (PSC) is a chronic fibrotic cholangiopathy that affects intra- and extrahepatic bile ducts. A PSC diagnosis occurs predominantly in men, with a median age of 30-40 years, and is oftentimes coexistent with inflammatory bowel disease.[3,4] Due to a lack of effective medical therapies, liver transplantation is the only curative option for advanced-stage PSC, with 5-year survival rates of around 70%.[1] However, organs are in short supply, and currently three people per day will die waiting for a viable liver. Furthermore, roughly 25% of PSC patients who receive a liver transplant

will experience pathological reoccurrence. These patients also have an increased risk of cholangiocarcinoma and colorectal cancer.[5] Further complicating medical management of PSC is episodic cholangitis and portal hypertension.[6]

It is not uncommon for PSC to progress silently, with up to 50% of PSC patients presenting as asymptomatic. Serologically, an elevation in alkaline phosphatase may be the only abnormal biochemical level present in a panel. However, this is not a reliable marker of disease progression or severity as liver enzyme fluctuations are common and may fall within normal parameters.[6] In addition to serological variations, patients with more advanced disease report an increase in overall fatigue, pruritus, hepatic pain, and tenderness in the upper right abdominal quadrant.[3,7]

Cholangiocytes

Cholangiocytes, the target cell of cholangiopathies such as PSC, comprise only 3-5% of cellular residents in healthy liver tissue. These cells are heterogeneous in nature, differing in their physical appearance, geographical proximity, and biological functions. Deep within the liver lie the canals of Hering, where canicular bile is transported from the apical membrane of the hepatocytes to the portal tracts for further modification by resident cholangiocytes.[8] Cholangiocytes secrete various ions through hormone regulation to modify the bile as it flows through the biliary tree.

The biliary tree, aptly named for its branching hepatic protrusions, exists both inside and outside the liver. The intra-hepatic portion begins with microscopic ductules that emerge from Hering's canals and are lined entirely by cholangiocytes. The diameter of the ductules increases as the bile travels further away from its hepatic source. Interlobular ducts then converge into septal ducts. From there, bile travels through area

ducts and segmental ducts where the trunk is joined by first the right and then the left hepatic duct as the biliary tree exits the liver and the common bile duct eventually empties its contents into the duodenum.[9]

The ducts of the biliary tree, first divided into intra- and extrahepatic ducts, are further divided into both small (<15 μm) and large (>15 μm) intrahepatic bile ducts. Cholangiocytes respond to differences in diameter with variations in their morphological, phenotypical, and biochemical responses. Cholangiocytes lining the small bile ducts, or those less than 15 μm in diameter, are referred to as small cholangiocytes. These cells tend to be more cuboidal in shape and have a higher nucleus to cytoplasm ratio when compared to their larger cohorts.[10-12] Large cholangiocytes, which line the large bile ducts, are more columnar, ciliated, and have internal organelles and organization not found in their smaller counterparts. Additionally, large cholangiocytes, but not the small, will express various receptors such as the secretin receptor, somatostatin receptor, anion exchanger 2, and cystic fibrosis transmembrane conductance regulator. Large cholangiocytes' proliferative and secretory pathways respond to signaling changes in cyclic adenosine 3',5'-monophosphate (cAMP), whereas the primary regulation of small cholangiocytes is mediated by the IP_3 (D-*myo*-inositol 1,4,5-trisphosphate)/Ca^{2+}/calmodulin-dependent protein kinase I pathway.[10,13,14] These independent pathways provide for differing responses to insult or injury. It has been previously shown that large but not small cholangiocytes respond with an increase in biliary mass in response to activated cAMP signaling.[15,16] One of the most well-studied modification pathways is the secretin (SCT)/secretin receptor (SR) pathway, whereby through the binding of secretin to the secretin receptor located on the basolateral

membrane, cAMP forms, leading to the expulsion of chloride ions into the luminal space, creating a concentration gradient that activates bicarbonate anion exchanger 2 allowing for the passive movement of water and the absorption of bile salts, amino acids, and glucose.[17,10]

PSC Pathology

As previously noted, PSC is a complex hepatic pathology involving a myriad of processes and pathways. Due to the idiopathic nature of PSC, there is currently no definitive diagnostic test. Patients with PSC may have elevated serum alkaline phosphatase, serum aminotransferase, or IgG levels, although some patients will present with these biochemical tests within normal parameters.[18,19] During PSC progression, cholangiocytes play various roles, contributing to the different pathological phenotypes commonly found within the hepatic microenvironment.

Ductular Reaction

Ductular reaction is the hepatic phenomenon in which the injured liver compensates by increasing the number of ductules and matrix deposition through hepatic adult stem-like cells and an increased immune cell presence, leading to periportal fibrosis and cirrhosis. Research has shown ductular reaction differs from canonic regeneration by relying on the activation of biliary epithelial cells, termed hepatic progenitor cells, instead of hepatocyte-mediated regeneration.[20] In addition to immune cell activation, ductular reaction matrix deposition in PSC patients coincides with increased expression of extracellular matrix (ECM) genes, including Col1a1 and Fn1.[21]

Hepatic Fibrosis

Hepatic fibrosis is a direct result of the biological imbalance between the deposition and break down of the ECM. Hepatic fibrosis is a necessary step in the restoration of the normal parenchyma following insult or injury. However, during chronic liver diseases, such as PSC, multiple pathways will contribute to hepatic stellate cell (HSC) activation, resulting in an overproduction of ECM that, left unchecked, leads to the formation of nodules, altered blood flow, and permanent scarring.[22] HSCs have long been identified as critical players in liver fibrogenesis, moving from a quiescent state where they act as a vitamin A and fat storage vessel to an activated myofibroblast phenotype that actively participates in the deposition of collagen.[23,24] Due to intense research in the field of liver fibrogenesis, scientists now know that while the HSC is a primary player in liver fibrosis, it acts in concert with a host of other cells within the hepatic environment creating a complex network of pathways, thereby reducing the efficacy of a single target or treatment.

Angiogenesis

Angiogenesis is the formation of new blood vessels from preexisting vessels within a tissue or organ, typically responding to hypoxic or inflammatory conditions. In functional tissues, a delicate balance between pro- and anti-angiogenic factors supports a largely quiescent microenvironment that is disrupted during hypoxic and inflammatory conditions such as cancer and fibrosis.[25,26] During inflammation, vascular permeability increases, and chemokine production from the surrounding environment draws a variety of pro-angiogenic immune cells such as monocytes, macrophages, and mast cells.[27] These cells secrete factors such as angiogenin, transforming growth factor beta1 (TGF-β1), and interleukin-6 (IL-6) that activate angiogenic pathways.[28] Previous research has

demonstrated treatment with angiogenic inhibitors such as tyrosine kinase inhibitors reduces liver fibrosis in a rat model of portal hypertension.[29]

Inflammatory Response

PSC is marked by both fibrosis and inflammation. These two key elements impair bile formation and flow, progressing liver dysfunction towards cirrhosis and creating a malignant microenvironment.[30] Liver injury activates resident immune cells, such as Kupffer cells, along with circulating lymphocytes, neutrophils, and dendritic cells. These cells further activate HSCs, resulting in increased production and deposition of collagen.[31] This cycle is initiated and exacerbated by the cholangiocytes, who take on a neuroendocrine phenotype in response to hepatic injury, interacting with the surrounding environment through pro-inflammatory mediators such as tumor necrosis factor alpha and IL-6. These cytokines then act in both an autocrine and paracrine fashion, further activating cholangiocytes and neighboring HSCs.[32]

Biliary Senescence

Another important hallmark of PSC is biliary senescence. Senescence is a fascinating phenomenon whereby healthy cells, in response to endogenous or exogenous stressors, enter a state of permanent arrest. These include a variety of triggers such as DNA damage, repair processes, or oncogenic activation.[33] Unlike quiescence, which is a reversible phase G1, p270-associated cyclin-dependent kinase (CDK) inactivation response, senescence depends on either p16 or p21 CDK inactivation, is irreversible and may occur in either phase G1 or G2 of the cell cycle.[34] Although senescent cells cannot proliferate, they remain metabolically active and participate in regional signaling, often influencing neighboring cells. Senescing cells also undergo variation in genetic

expression when compared to their functional counterparts, including an increase in CDK inhibitors p16 and p21.[35] PSC patients have significantly increased numbers of senescent cells, when compared to normal controls, as demonstrated by Laish *et al*., further increasing the odds of developing hepatic malignancies later in life.[36]

One way that senescent cells participate in the regulation of the hepatic microenvironment is through the acquisition of a senescence-associated secretory phenotype, or SASP. SASP has a duplicitous role within the organism, working first to promote an immunological response to tumorigenic cells, stimulate wound healing, and aid in tissue regeneration. As the organism ages, this secretory phenotype can contribute to chronic inflammation, support a malignant environment, and increase angiogenesis.[37]

Animal Models of PSC

Currently, no one mouse model comprises a majority of PSC pathologies, further adding to the current challenges of elucidating novel treatment options. Ideally, an animal model will mimic the most common characteristics of PSC, such as bile duct hyperplasia, strictures, liver enzyme panel abnormalities, inflammation, cirrhosis, and cholestasis.[38,39] Murine models can be further separated into mechanical injury models, chemical injury models, and genetic modification models.

Mechanical Injury Mouse Models

The most common mechanical injury model for PSC is the bile-duct ligation (BDL) mouse model. In this model, healthy young animals, typically male, undergo abdominal surgery in which the peritoneal cavity is exposed, the liver is lifted, and the common bile duct exposed. The bile duct is then separated from the hepatic artery and the portal vein before 5-0 suture is used to tie off the bile duct in two locations, one above the other.

Following abdominal closure and recovery, the animal will develop serum markers common in hepatic injury, an influx of inflammatory cells, and the deposition of collagen through the parenchyma. Within two weeks, liver protein extracts display marked increases in collagen, type I, α-SMA, vimentin, and oncogene LCN2, as shown through western blotting.[40] A significant drawback to this acute mechanical injury is the rapidity by which the liver undergoes functional and pathological changes. Contrary to PSC, a chronic, long-term hepatic pathology of unknown origin, BDL is an acute, rapid onset mechanical injury better suited to modeling cholangiocyte proliferation, portal pressure, and extrahepatic cholestasis.[41]

Chemical Injury Mouse Models

Due to the limitations of mechanical injury in a chronic setting, chemical models were developed. One standard, well-developed model is the 3,5-diethoxycarbonyl-1,4-dihydrocollidine (DDC) feeding mouse model. This model relies on regular DDC feeding from 1 to 8 weeks, based upon the severity of the injury and desired outcome. After four weeks, DDC-fed animals develop onion-skin fibrosis, a characteristic finding in PSC patients.[42] In contrast to the mechanical blockage caused by the tying off of the common bile duct, continuous exposure to a DDC diet inhibits ferrochelatase, a mitochondrial enzyme that catalyzes the formation of heme from ferrous iron and protoporphyrin. Protoporphyrin is poorly soluble and consequently precipitates in the canaliculi and bile ducts.

In addition to onion-skin fibrosis, DDC feeding increases infiltrating mononuclear cells, activated myofibroblasts, and pericholangitis. However, a significant downfall to the DDC feeding model is the lack of immune components found in human patients, often in

the form of fibro-obliterative lesions.[43] Another chemically induced state of sclerosing cholangitis is the lithocholic acid (LCA) mouse model. In this model, Swiss albino mice are fed a 1% (w/w) LCA diet for either 1, 2, or 4 days. Like the DDC model, physical obstruction within the ducts, in the form of crystals, causes injury to the biliary epithelial cells, or cholangiocytes. Similar to human pathology, serum alanine aminotransferase increases along with alkaline phosphatase and bilirubin levels are elevated. Electron microscopy has revealed tight junction disruption and reduced expression of ZO-1. On par with BDL mice, α-SMA protein was present in more significant amounts than controls, along with Ki-67-positive periductal cells.[44] Unfortunately, as with mechanical injury, LCA is a rapid-onset disease state that, due to its aggressive nature, results in extreme mortality at >90% at two weeks, rendering it unsustainable for long-term chronic studies.[45] Due to the complications with chemical injury models, researchers must look to other routes to better model PSC.

Genetic Injury Mouse Model

One of the more popular genetically modified mouse models for PSC is the *Abcb4*$^{-/-}$ model on an FVB/NJ background. These mice, referred to as Mdr2$^{-/-}$, express orthologs to the human gene Mdr3, both of which code for a phospholipid transporter of canicular origin. These ABC transporters act as flippases that remove individual phospholipids from the outer leaflet of the membrane to the extracellular space. There they are taken up by monomers of bile salts that interact with one another to create a micelle within the extracellular space. The micelles further rearrange to incorporate cholesterol, which is secreted by the ABC transporters Abcg5 and -8. These micelles provide a protective element to the hepatocyte bilayer membrane against the toxic nature of the bile salts.[46]

The bile of Mdr2 knockout mice lacks phosphatidylcholine and exhibits lower levels of secreted cholesterol. This absence of canalicular phospholipid flippase then results in the spontaneous development of hepatic injury, in the form of an increase in collagen deposition within the liver parenchyma, bile duct proliferation, disruption of tight junctions, and increased angiogenesis.[47] The main criticism of the $Mdr2^{-/-}$ mouse model as a model of PSC is that in later stages these animals will consistently develop hepatocellular carcinoma, indicating the activated pathways within the model are not representative of the human connection between PSC and cholangiocarcinoma (CCA).[48]

A connection has previously been established between individuals with inflammatory bowel disease and some form of cystic fibrosis gene (CFTR) mutation and the later development of PSC. To model this, genetically modified mice (CF) with either homozygous and heterozygous mutations in the CFTR gene were given either Peptamen or Peptamen plus dextran sodium sulfate (DSS) for periods of 7 to 21 days to induce biliary injury. While the standard protocol is to provide DSS in the animal's drinking water, CF mice consume varying amounts of water throughout the day. To normalize the doses among the groups, Peptamen was used as a carrier. DSS statistically increased alkaline phosphatase levels, bile duct proliferation, and inflammatory infiltrate.[49] However, despite the many similarities to human liver pathology, CF mice are lacking in crucial areas. Unlike their $Mdr2^{-/-}$ counterparts, CF mice do not spontaneously develop liver fibrosis at early ages and thus researchers must either rely on chemical injury stimulation or breed older animals and wait longer for pathological findings. Also, CF mice are at higher risk for developing intestinal obstruction and must rely on liquid feeding upon weaning.[50]

Alternative Models

Aside from the standard murine models, there are two uncommon animals that naturally develop sclerosing cholangitis that may be useful in teasing out the underlying etiology of PSC. The first animal of note is the ordinary house cat. Similar to human pathology, feline cholangitis is a slow-developing, inflammatory disease that results in increased serum liver enzymes and fibrosis of the bile ducts. Although the root cause of feline cholangitis may be of bacterial origin, or due to liver flukes, pancreatitis, or inflammatory bowel disease, a large percentage of these cases have no known cause. [51] While these animals are not traditionally used in PSC research, feline cholangitis may prove to be a valuable translational model for human sclerosing cholangitis. [52] The last model of note is baboon sclerosing cholangitis. While extremely rare, research has recorded two cases of male baboons spontaneously developing sclerosing cholangitis with increased serum liver enzymes, inflammatory infiltrate, ductular proliferation, and fibrosis. These baboons were both males, further reflecting the prevalence of PSC in male homo sapiens. Similarly, it is agreed that PSC is a product of both genetic and environmental factors, and while these baboons were not related, they were both part of the same dietary research group in southwest Texas. While this disease was not induced in these animals, and they are not bred to be PSC research animals, their spontaneous disease more closely matched the histopathological features of human PSC than has been previously seen. Their tissues may offer insight into PSC that we cannot find in the models mentioned above. [53]

Fibroblast Growth Factors

Fibroblast Growth Factor 1

Fibroblast growth factor 1 (FGF1) belongs to a family comprised of twenty-three structurally related proteins that regulate various biological functions, including growth, proliferation, migration, and survival.[54] Members of the FGF family signal through a group of four tyrosine kinase receptors consisting of a single α-helix spanning the membrane, three subdomains protruding into the extracellular space, and an intracellular tyrosine kinase domain. Activation of the intracellular domain is commonly achieved by extracellular binding of the FGF.[55,56] Dimerization follows binding of the ligand to the receptor, inducing transautophosphorylation, which results in the activation of downstream pathways. Activation of the FGF receptor (FGFR) by either paracrine or autocrine sources of FGF relies upon the presence of heparan sulfate. Heparan sulfate is a crucial component of the FGF-FGFR complex, linking an FGF to domain 2 of the FGFR chain, thereby stabilizing the complex and increasing the interaction between the ligand and its receptor.[57] In contrast to the remaining members of the FGF family, FGF1 and -2 lack the hydrophobic amino acids at the N-terminus of the peptide that are necessary for trafficking to the endoplasmic reticulum. From here, the secretory proteins are further transported to the Golgi apparatus to be packaged into vesicles for extracellular secretion.[58,59] Instead, members of the FGF1 subfamily are transported directly across the cell membrane using a complex consisting of S100A13 and synaptotagmin-1. FGF1 has also been found within the cell nucleus, where it is believed to regulate differentiation and apoptosis.[60] Once released from the cell's interior, FGF1

alone can bind to and activate any of the four FGFR subtypes. This unique characteristic allows FGF1 to exert its influence in every tissue and organ system within the organism.

Benefit, Dysfunction, and Disease

FGF1 plays a duplicitous role within the body, functioning protectively in various conditions such as type 2 diabetes mellitus, hepatoxicity, wound healing, and homeostasis, among others. Conversely, FGF1 has also been implicated in inflammatory conditions such as psoriasis, rheumatoid arthritis, and colorectal cancer.

Type 2 diabetes affects more than 400 million adults worldwide, having nearly doubled in the last three decades, creating a financial burden and healthcare crisis. Recently, it has been found that FGF1 plays an active role in glucose control in diabetic rodents, where just a single injection of FGF1 lowered blood glucose levels within seven days and continued to exert those benefits at the four-month mark.[61] In addition to participation in glucose regulation, research has demonstrated a protective role for FGF1 in acetaminophen (APAP)-induced injury in C57BL/6 mice. FGF1 was injected intraperitoneally following APAP injections of 500 mg/kg body weight. Compared to non-treated APAP-injured animals, FGF1 treatment lowered levels of inflammatory cytokines, oxidative damage, and ER stress suggested to contribute to hepatic necrosis.[62] FGF1 has also been shown to benefit wound healing when combined with fibroin hydrogels in a rat model of full-thickness skin excision. FGF1 presence alone was sufficient to significantly increase proliferation and migration of fibroblast L929 cultured cells when compared to silk fibroin alone, but the combination of silk fibroin with FGF1 more than doubled the ability of cells to migrate and proliferate, which not only also significantly increased wound healing in the rat model, but also reduced the overall amount of scar

tissue deposition at day 23.[63] In addition to its previous roles, FGF1 has also been shown to participate in metabolic homeostasis through the PPARγ-FGF1 axis. Jonker *et al.* discovered that FGF1 knockout mice, while phenotypically normal, responded to high-fat diet feedings with an aggressive diabetic response, which failed to resolve upon reintroduction to regular chow. They further reported that the regulatory mechanism necessary for metabolic homeostasis was PPARγ acting through the FGF1 gene. Loss of functionality of this gene, or expression of FGF1, increased hepatic steatosis and insulin resistance. [64]

In contrast to the beneficial role FGF1 plays in type 2 diabetes, research has identified FGF1 as a participant in various disease states, such as psoriasis. Psoriasis is an inflammatory skin condition, that includes hyperplasia and scaling, in which elevated levels of IL-26 have been shown to increase the expression of FGF1, -2, and -7. Further analysis of normal human epidermal keratinocytes linked FGF1 to IL-26 in a dose-dependent manner. [65] FGF1 has also been implicated in the participation of bone loss during periods of active inflammation in patients suffering from rheumatoid arthritis. Rheumatoid arthritis is an autoimmune disorder characterized by leukocyte and macrophage migration to the synovial fluid that results in irreversible destruction of bone and cartilage. In addition to vascular endothelial growth factors, FGF1 has been identified as a critical player in rheumatoid arthritis pathology. FGF1 increases synoviocyte proliferation and overall angiogenesis, while activation of FGFR1 regulates bone resorption. [66] Similar to the previous conditions, FGF1 participates in ulcerative colitis, an inflammatory disease of the digestive tract that significantly increases the patient's risk of colorectal cancer. Cancer-associated fibroblasts have been shown to secrete FGF1,

which promotes tumorigenesis. Tumor cells isolated from patient samples showed increased levels of FGF1 and -3, which perpetuated the autophosphorylation of FGFR4. This stimulation resulted in mitogen-activated protein kinase activation, among others, which in turn promoted colorectal cancer cell growth. [67]

Despite the role FGF1 plays in various pathologies, global FGF1 knockout mice exhibit normal phenotypes and functionality. However, numerous disease states are associated with FGFR mutations, such as Pfeiffer syndrome, Apert syndrome, and achondroplasia, to name but a few. [68]

miRNA

MicroRNAs were first discovered over 40 years ago in *C. elegans* when researchers found what they thought was a traditional protein code but instead discovered a small RNA sequence that coded for a regulatory nucleotide. [69,70] These sequences, coined microRNAs (miRNAs), are typically only 20-23 nucleotides in length, and their primary function is to regulate the protein expression through either translational interference or degradation. In the canonical pathway, miRNAs arise from intron sequences and after transcription are processed by a complex that includes a binding protein and Drosha enzyme. This complex cleaves the base of hairpin to allow for exportation into the cytoplasm for further processing by an endonuclease called Dicer. [71] From here, argonaute family proteins help to form RISC (RNA-induced silencing complex) which through conformational change separates the miRNA into two strands and discards the unwanted, or passenger, strand. [72]

miRNA's are not specific for one mRNA, and one miRNA may have the ability to target dozens, if not hundreds of mRNA molecules. [73] These individual regulators of gene expression can regulate a host of biological functions such as proliferation, metabolism, apoptosis, development, and migration.

miR-16

The microRNA miR-16 is part of the miR-15 family of microRNAs located on chromosome 13 between exons 4 and 5 of the reverse strand. [74] Members of the miR-15 family have been identified as tumor suppressors with anti-angiogenic properties. [75] As a result, these microRNAs are often the targets of deletion or dysregulation in various pathologies such as cancer. [76,77]

Dysfunction and Disease

miR-16 has been implicated not only in cancers but also in a variety of autoimmune diseases as well. [78] Normal expression of miR-16 inhibits cellular proliferation and inflammation by targeting PDCD4, which suppresses inflammatory macrophages. [79] One significant autoimmune disorder in the scope of PSC is inflammatory bowel disease. Inflammatory bowel disease encompasses both ulcerative colitis and Crohn's disease. Recent studies have shown a strong correlation between disease activity and fecal miR-16 levels suggesting the viability of miR-16 as a marker of disease pathology. [80]

miR-16 also plays a role in hepatic fibrosis. During disease or injury, HSCs transform from their normally quiescent phenotype where they function to store retinyl esters to myofibroblasts, an actively proliferating, contractile, inflammatory cell whose job is the deposition of collagen fibers within the parenchyma. [81] Research in rodents has

demonstrated a significant deficiency in miR-16 levels in myofibroblasts when compared to HSCs. Restoration of basal miR-16 levels resulted in a downregulation in collagen type I and III production. [82]

A key element of PSC is the proliferation of the bile ducts in response to the altered microenvironment. This is identified through an increase in cytokeratin-19- (CK-19-) positive cells present in the ductules throughout the biliary system. [83] Samples of human hepatocellular carcinoma have been shown to have significant decreases in miR-16, and subsequent testing has indicated miR-16 mimics may reduce the proliferative capacities of these tumor cells. [84]

Based upon the previous literature regarding the role of FGF1 in inflammation, proliferation, and angiogenesis, along with the duplicitous role FGF1 plays in various pathologies, we proposed the following specific aims: (i) to evaluate the role that FGF1/FGFRs play in the ductular reaction, fibrosis, and inflammation in a mouse model of PSC; (ii) to evaluate the effect of inhibition of FGF1/FGFRs on biliary proliferation, fibrosis, inflammation, and senescence in a mouse model of PSC; and (iii) to determine the role that miR-16 plays in concert with FGF1/FGFR activation or inhibition. Our studies provide evidence that FGF1 is upregulated in our injury models, and administration of recombinant human FGF1 (rhFGF1) further exacerbated the inflammation, proliferation, and fibrosis in the BDL animals. Conversely, treatment with a pan FGFR antagonist lowered the injury parameters in both the acute and chronic injury models and increased miR-16 compared to controls. Therefore, modulation of the FGF1 axis may provide a novel treatment in the fight against cholangiopathies such as PSC.

CHAPTER II MATERIALS AND METHODS

Materials

Immunohistochemistry supplies and reagents for tissue culture were obtained from ThermoFisher Scientific (Waltham, MA). Animals were treated with a recombinant human FGF1 protein (rhFGF1, fibroblast growth factor acidic protein, GF002, Millipore Sigma), a mouse FGF acidic/FGF1 neutralizing antibody (AF4686, R&D Systems, Minneapolis, MN),[85] or a pan FGFR antagonist (AZD4547, ab216311, Abcam, Burlington, CA).[86] Total RNA was isolated using the *mir*Vana miRNA Isolation Kit (Invitrogen, Carlsbad, CA) and reverse-transcribed with an iScript Reverse Transcription Kit from Bio-Rad Laboratories (Hercules, CA). miRNA cDNA was synthesized with a Taqman™ Advanced miRNA cDNA Synthesis Kit (A28007, ThermoFisher Scientific). The antibodies against CK-19 (ab52625), desmin (ab185033), F4/80 (ab6640), FGFR1 (ab10646), FGFR2 (ab10648), FGFR3 (ab180906), FGFR4 (ab44971), p16 (ab211542) as well as enzyme-linked immunosorbent assay (ELISA) kits for FGF1 (ab226587) and TGF-β1 serum analysis (ab119557) were purchased from Abcam. The FGF1 Alexa Fluor 555-conjugated antibody (bs-0229R-A555) was purchased from Bioss Antibodies (Woburn, MA). The angiogenesis (ANG) antibody (SC-74528) was purchased from Santa Cruz Biotechnology (Dallas, TX). CD31 (NB-100-1642) antibody came from Novus Biologicals (Centennial, CO). The senescence associated-β-galactosidase (SA-β-Gal) staining kit was purchased from Cell Signaling Technology (Boston, MA). Primer information is listed in Table 1.

Table 1: List of mouse and human primers used.

Gene	Species	Detected Transcript	Source
α-SMA	Mouse	NM_007392	Qiagen
ANG	Mouse	NM_007447	Qiagen
CDKN1a (p21)	Mouse	NM_007669	Qiagen
CDKN2a (p16)	Mouse	NM_009877	Qiagen
Col1a1	Mouse	NM_007742	Qiagen
FGF1	Mouse	NM_010197	Qiagen
FGFR1	Mouse	NM_010206	Qiagen
FGFR2	Mouse	NM_010207	Qiagen
FGFR3	Mouse	NM_008010	Qiagen
FGFR4	Mouse	NM_008011	Qiagen
GAPDH	Mouse	NM_008084	Qiagen
IL-1β	Mouse	NM_001314054	Qiagen
IL-6	Mouse	NM_008361	Qiagen
Ki67	Mouse	NM_001081117	Qiagen
miR-16	Mouse	477860_mir	Thermo Fisher
miR-control	Mouse	mmu481815_mir	Thermo Fisher
PCNA	Mouse	NM_011045	Qiagen
PECAM (CD31)	Mouse	NM_008816	Qiagen

Table 2: List of mouse and human primers used (continued).

TGF-β1	Mouse	NM_011577	Qiagen
TRP53 (p53)	Mouse	NM_011640	Qiagen
VEGFA	Mouse	NM_009505	Qiagen
ANG	Human	NM_001145	Qiagen
CDKN1a (p21)	Human	NM_000389	Qiagen
CDKN2a (p16)	Human	NM_000077	Qiagen
Col1a1	Human	NM_000088	Qiagen
FGFR1	Human	NM_015850	Qiagen
FGFR2	Human	NM_000141	Qiagen
FGFR3	Human	NM_000142	Qiagen
FGFR4	Human	NM_002011	Qiagen
FN-1	Human	NM_002026	Qiagen
GAPDH	Human	NM_002046	Qiagen
IL-1β	Human	NM_000576	Qiagen
IL-6	Human	NM_000600	Qiagen
Ki67	Human	NM_002417	Qiagen
PCNA	Human	NM_182649	Qiagen
miR-16	Human	478727_mir	Thermo Fisher
miR-control	Human	478323_mir	Thermo Fisher
MCP-1	Human	NM_002089	Qiagen
TGF-β1	Human	NM_000660	Qiagen

Animal Models

All animal procedures were performed following protocols approved by the Texas A&M University Institutional Animal Care and Use Committee. Male C57BL/6 (25-30 g), wild-type (WT) mice, and FVB/NJ (control for $Mdr2^{-/-}$ mice) were purchased from Jackson Laboratories (Bar Harbor, ME). Male $Mdr2^{-/-}$ mice came from in-house breeding colonies established at the Texas A&M University College of Medicine, originating from mice purchased from Jackson Labs. All mice were housed in a temperature-controlled environment, with 12:12 hour light-dark cycles with access *ad libitum* to water and standard mouse chow. C57BL/6 mice underwent BDL as described [87] with minipump implantation occurring post ligation. In accordance with previous rodent research, WT and BDL mice received minipumps delivering either recombinant human FGF1 (100 mg/kg/day) [88,89,90] or AZD4547 (100 ng/kg BW/day).[86] At the age of approximately 12 weeks, male FVB/NJ and $Mdr2^{-/-}$ mice were treated with an FGFR antagonist (AZD4547, 100 ng/kg BW/day)[91] in sterile saline via an intraperitoneal Alzet® osmotic minipump for seven days, or anti-FGF1 monoclonal antibody (5 μg/100 μL saline)[85] via tail-vein injection [92] every other day for one week. Mice were euthanized either 7-days post-BDL or minipump implantation. Animals receiving monoclonal antibody treatment were euthanized 48 hours following final injections. Liver/body weight ratios were recorded (Table 2), and serum, total liver, and cholangiocytes were collected.

Table 3: Liver to body weight ratios.

	Liver weight (g)	Body weight (g)	Liver to body weight (%)
WT (n=10)	1.35 ± 0.47	26.35 ± 4.16	5.14 ± 2.11
WT + rhFGF1 (n=10)	1.76 ± 0.37	29.46 ± 7.43	5.71 ± 2.28
WT + AZD4547 (n=9)	1.62 ± 0.50	26.97 ± 7.25	6.29 ± 2.65
BDL (n=10)	1.54 ± 0.44	24.90 ± 6.96	6.26 ± 2.27
BDL + rhFGF1 (n=10)	1.47 ± 0.14	23.81 ± 1.53	6.15 ± 0.89
BDL + AZD4547 (n=9)	1.60 ± 0.38	24.13 ± 3.10	6.71 ± 0.26
FVB/NJ (n =10)	1.49 ± 0.49	28.65 ± 2.39	5.19 ± 1.19
FVB/NJ+ AZD4547 (n = 12)	2.01 ± 0.50	29.23 ± 2.90	6.93 ± 2.24*
FVB/NJ + anti-FGF1 mAb (n = 9)	1.54 ± 0.40	28.71 ± 2.24	5.35 ± 1.37
$Mdr2^{-/-}$ (n = 10)	3.32 ± 0.61	30.97 ± 2.84	10.76 ± 2.32*
$Mdr2^{-/-}$ + AZD4547 (n = 9)	1.59 ± 0.49	27.87 ± 3.09	5.67 ± 1.57#
$Mdr2^{-/-}$ + anti-FGF1 mAb (n = 9)	2.14 ± 0.65	29.48 ± 3.71	7.26 ± 2.78#

*p<.05 vs. Normal or WT mice.

#p<.05 vs. $Mdr2^{-/-}$ mice.

Isolation of cholangiocytes

Virtually pure preparations of murine cholangiocytes were isolated as described using immunoaffinity separation. [93] The antibody utilized recognizes an unidentified antigen expressed by all intrahepatic cholangiocytes (IgG_{2a}, a gift from Dr. R. A. Faris, Brown University, Providence, RI). Following isolation, a portion of isolated cholangiocytes was counted, resuspended, and placed in a shaking water bath for 6 hours before the cells were spun down and the supernatant was removed and stored for later use in various ELISAs.

Immunoreactivity/expression of FGFR1-4 and FGF1 and measurement of FGF1 levels in serum and cholangiocyte supernatants

We evaluated: (i) the immunoreactivity of FGFR1-4 and FGF1 in frozen liver sections (5 μm thick, six sections, four randomized animals from each treatment group) co-stained with markers of cholangiocytes (CK-19) [94] or HSCs (desmin); [95] (ii) FGF1 levels in serum and cholangiocyte supernatants from selected treatment groups (n=9) by ELISA; and (iii) mRNA expression of FGFR1-4 and FGF1 (normalized to glyceraldehyde-3-phosphate dehydrogenase, GAPDH) by *q*PCR in three isolated, purified cholangiocyte preparations from selected groups of animals (n=3 each preparation). When possible, control and treatment sections were mounted on the same slide for consistency in staining. If sections could not be mounted together, all staining was done concurrently, to maintain environmental consistencies. Negative controls consisted of sections stained with secondary antibody only. Images were visualized using an Olympus Fluoview FV3000 Confocal Scanning Microscope (Integrated Microscopy Imaging Laboratory,

Texas A&M); *q*PCR was performed on a QuantStudio 6 Flex Real-Time PCR System (ThermoFisher Scientific).

Measurement of intrahepatic bile duct mass (IBDM) and biliary proliferation

IBDM was measured in either paraffin-embedded (WT and BDL mice) or frozen liver sections (FVB/NJ and Mdr2$^{-/-}$ mice) by immunostaining for CK-19-positive areas (5 μm thick, two slides, ten fields per group from 9 animals), which was quantified using VisioPharm software, version 2018.09 (Westminster, CO). [96] The mRNA expression of proliferation markers (proliferating cellular nuclear antigen, PCNA, and Ki67, normalized to GAPDH) was measured in cholangiocytes from the selected groups of animals by *q*PCR (3 cumulative cholangiocyte preparations [n=3 per preparation] for a total of 9 animals, n=9). [96]

Evaluation of liver fibrosis and miR-16 expression

Collagen deposition was evaluated by Sirius Red staining in paraffin-embedded liver sections (5 μm, ten fields of view from 9 animals per group) and quantified using VisioPharm software. Markers of liver fibrosis (α-SMA; Col1a1; and TGF-β1, normalized to GAPDH) were measured by *q*PCR in total liver samples from the selected groups of animals (3 cumulative cholangiocyte preparations, n=9). [97] TGF-β1 serum levels were determined using a commercially available ELISA kit (Abcam). Since miR-16 is downregulated in HSCs and contributes to the progression of liver fibrosis,[98] we measured biliary miR-16 expression (normalized to U6) by *q*PCR.[99]

Measurement of biliary senescence and liver inflammation and angiogenesis

Macrophage presence was analyzed by evaluating the number of F4/80-positive cells in paraffin-embedded liver sections (5 μm thick, ten fields from 9 animals) and quantified using VisioPharm software.[100] SA-β-Gal staining was performed in frozen liver sections (10 μm thick, six fields of view from 4 animals) using a commercially available SA-β-Gal staining kit (Cell Signaling Technology) following the manufacturer's protocol and quantified with VisioPharm software. We measured by *q*PCR the mRNA expression of inflammatory cytokines (IL-1β and IL-6)[101] and senescence markers (p21, p16, and p53)[102] in isolated cholangiocytes from the selected groups of animals (3 cumulative cholangiocyte preparations, n=9 mice). GAPDH was used as a housekeeping gene. We evaluated angiogenesis by measuring the immunoreactivity of platelet-endothelial cell adhesion molecule 1 (CD31) by immunofluorescence in frozen liver sections (4-5 μm thick, ten fields of view from 4 animals) and mRNA expression of the angiogenic factors, VEGFA and angiogenin (ANG), and the endothelial cell marker CD31 (normalized to GAPDH) in total liver samples from the selected groups of animals (n=9 mice).

Ingenuity pathway analysis networks miR-16 with FGFR/FGF1

Using Qiagen's Ingenuity Pathway Analysis (IPA), relationships were identified between miR-16 and FGFR1 and FGF1. Results are shown as directional solid or dashed arrows indicating direct or indirect relationships with symbols representing kinases, growth factors, and mature miRNA.

In vitro studies in cell lines of human intrahepatic biliary cells (H69) and human hepatic stellate cells (HSCs)

We evaluated FGFR1, 2, 3, and 4 gene expression in the immortalized standard intrahepatic cell line H69 (a gift of Dr. Gregory Gores, Mayo Medical School, Rochester, MN)[103] and in HSCs[104] by RT-PCR. Human H69 and human HSCs (purchased from ScienCell Research Laboratories, Carlsbad, CA) were cultured in 6-well plates with medium containing 5% fetal bovine serum and allowed to grow to 70-80% confluency. Before measuring the expression of proliferation, senescence, fibrosis, and angiogenesis markers via *q*PCR, the 6-well plates were serum-starved overnight, then cells were treated for 24 h with rhFGF1 protein (Abcam, 10 pg/ml).

Human samples

Human liver tissue samples (OCT-embedded tissue blocks) from late-stage PSC patients (n=4) were obtained through Dr. Burcin Ekser under a study protocol approved by the Institutional Review Board at Indiana University School of Medicine, Indianapolis, IN. Tissues from healthy controls (OCT-embedded tissue blocks, n=4) were purchased from Sekisui Xeno Tech (Kansas City, KS). Information about human subjects can be found in Table 3.

The expression of FGF1 and corresponding receptors (FGFR1, 2, 3, and-4) was evaluated by immunofluorescence in liver sections (4-5 μm thick, co-stained with CK-19 or desmin, six fields of view from 4 samples) from healthy controls or PSC patients. Antibodies were diluted 1:100 in 5% donkey serum in 1x phosphate-buffered saline, containing sodium-chloride, potassium chloride, disodium hydrogen phosphate, and

potassium dihydrogen phosphate (PBS) overnight at 4°C. Antibodies specific for rat and human FGF1 (ab9588), mouse, rat, and human FGFR1 (ab829), mouse, rat, and human FGFR2 (ab10648), and human FGFR3 (ab180906) were purchased from Abcam, and mouse, rat, and human FGFR4 (11098-1-AP) from Proteintech (Rosemont, IL). We also assessed the expression of miR-16 by *q*PCR in total liver samples from healthy controls and late-stage PSC samples.

Statistical analysis

All data are expressed as the mean ± standard error of the mean (SEM). Differences between groups were determined using student's unpaired t-test for analysis of two groups and one-way analysis of variance (ANOVA) when more than two groups were analyzed, followed by the Tukey-Kramer post hoc test. A p-value of <0.05 was deemed significant.

Table 4: Human subject information.

Sample	ID	Gender	Age	Blood Type	Ethnicity
PSC	EB29	F	56	O	N/A
PSC	EB37	M	33	A	N/A
PSC	EB43	F	45	O	N/A
PSC	EB62	M	61	O	N/A
Healthy Control	H1255	F	56	N/A	African American
Healthy Control	H1293	F	52	N/A	Caucasian
Healthy Control	H1296	M	46	N/A	Caucasian
Healthy Control	H1299	F	17	PSC	Caucasian

N/A = Not available; PSC = Primary Sclerosing Cholangitis.

CHAPTER III RESULTS

Evaluation of FGF receptor immunoreactivity and *FGFR1-4* gene expression

FGFR1, 2, 3, and 4 were evaluated by immunofluorescent immunoreactivity in cryopreserved total liver OCT sections, costained with either desmin, (a marker of activated HSCs), or CK-19 (a marker of cholangiocytes) in either BDL or Mdr2$^{-/-}$ mice and their corresponding controls (Figures 1 and 2). There were increases in immunoreactivity in receptors 1 through 4 in the cholangiocytes, which was especially prevalent in receptor 3 of the BDL animals. HSCs had increased immunoreactivity in receptors 1, 2, and 4, and to a much lesser extent, receptor 3 when compared to the WT control tissue. There were increased numbers and sizes of bile ducts, and an increased presence of desmin^{+} HSCs in the BDL animals when compared to controls (Figure 1). Merged images show prominent purple colocalization of cholangiocytes and FGFR1.

In the Mdr2$^{-/-}$ model there is a similar trend of increased CK19 and desmin^{+} cells when compared to the FVB control with increased immunoreactivity in both HSCs and cholangiocytes of receptor 1 (Figure 2). Receptor 2 has no discernible immunoreactivity in the cholangiocytes in the control sample, yet there is clear staining in the HSCs. There is increased immunoreactivity in the Mdr2$^{-/-}$ sample when compared to the FVB, in both the HSCs and the cholangiocytes of FGFR2. Visually there appears to be no obvious immunoreactivity of receptor 3 in either the HSCs or cholangiocytes in the FVB control, which is only slightly increased in the Mdr2$^{-/-}$ animals. Receptor 4 immunoreactivity is increased in both cholangiocytes and HSCs in the knockout animals when compared to their FVB controls (Figure 2).

By *q*PCR, there was enhanced mRNA expression of *FGFR1, 2, 3,* and *4* in cholangiocytes from BDL and Mdr2$^{-/-}$ compared to control mice (Figure 3).

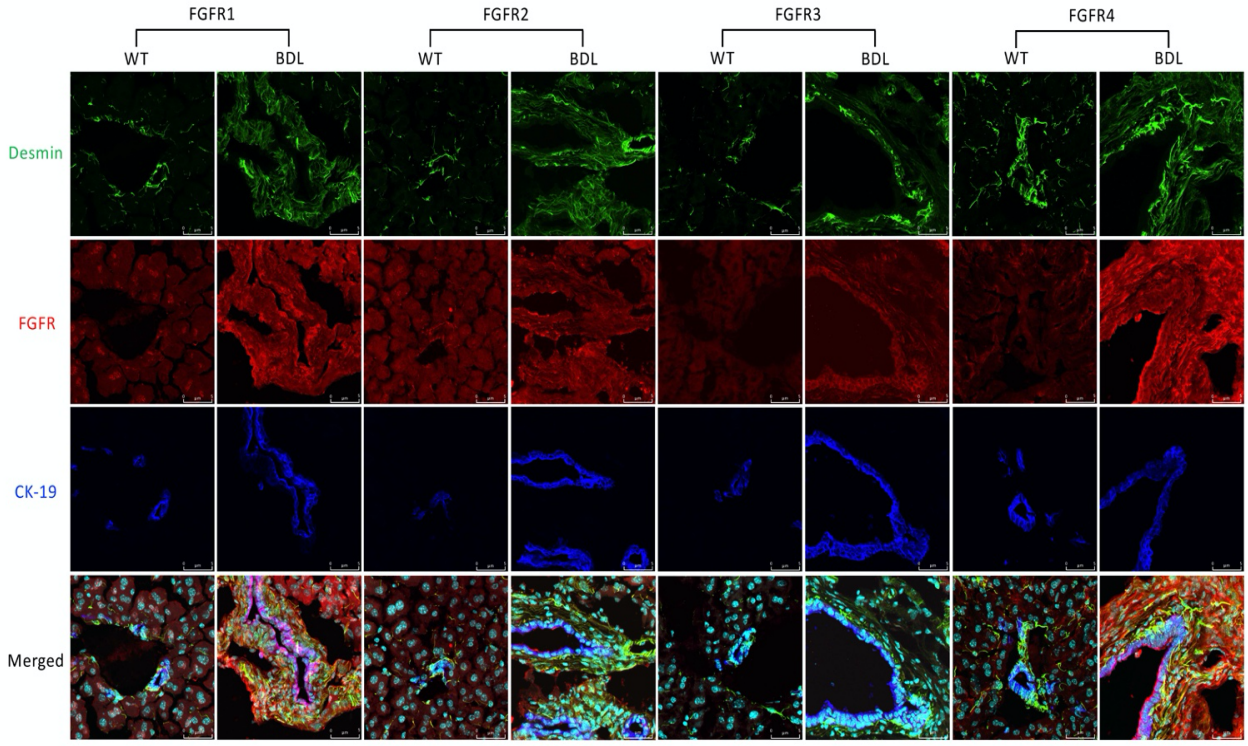

Figure 1: Immunoreactivity of cholangiocytes FGFR 1-4 in OCT liver sections from BDL and WT type mice

There was immunoreactivity of FGFR1-4 in cholangiocytes (co-stained with CK-19 antibodies) and at lower levels in HSCs (co-stained with desmin antibodies) in liver sections from C57BL/6 and BDL mice. Receptor expression was increased in BDL mice compared to the C57BL/6 control mice. Scale bar = 5 μm.

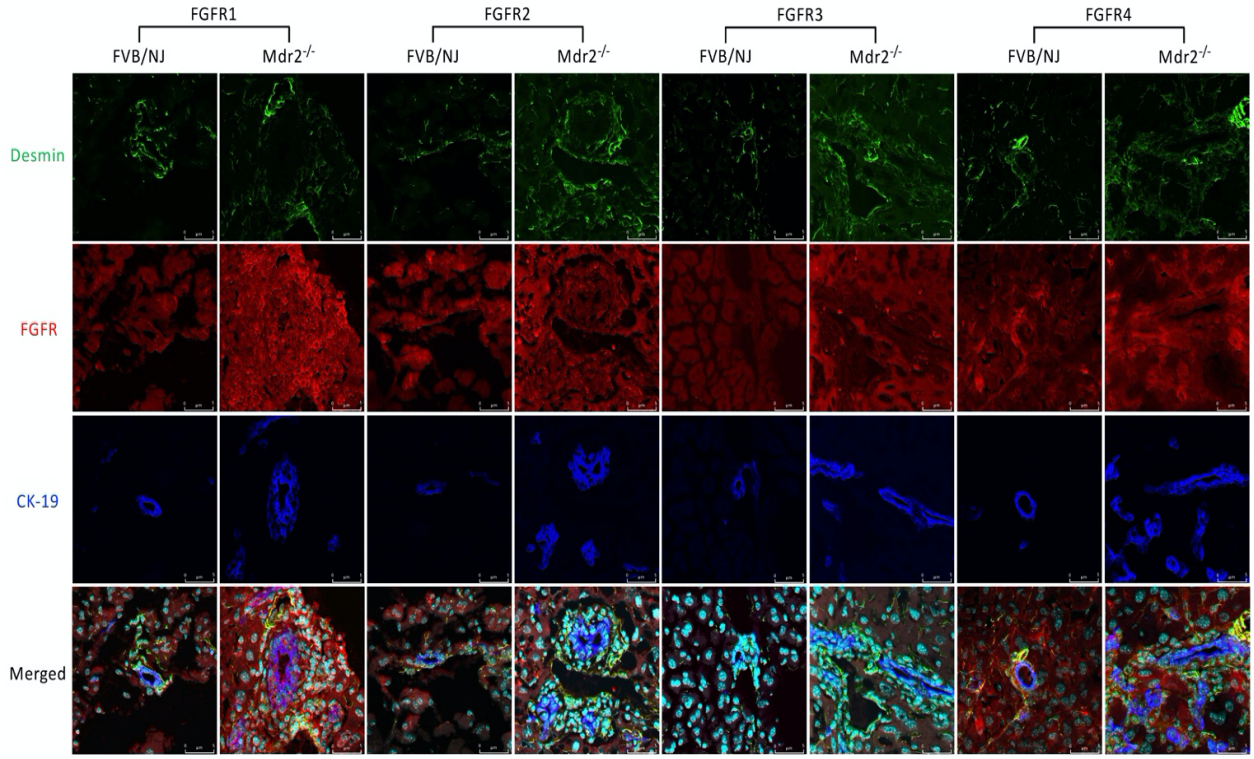

Figure 2: Evaluation of FGFR 1-4 in OCT liver sections from Mdr2$^{-/-}$ and FVB controls

There was immunoreactivity for FGFR1-4 in cholangiocytes and at lower levels in HSCs (co-stained with CK-19 and desmin, respectively) in liver sections from both FVB/NJ and Mdr2$^{-/-}$ mice. Scale bar = 5 μm.

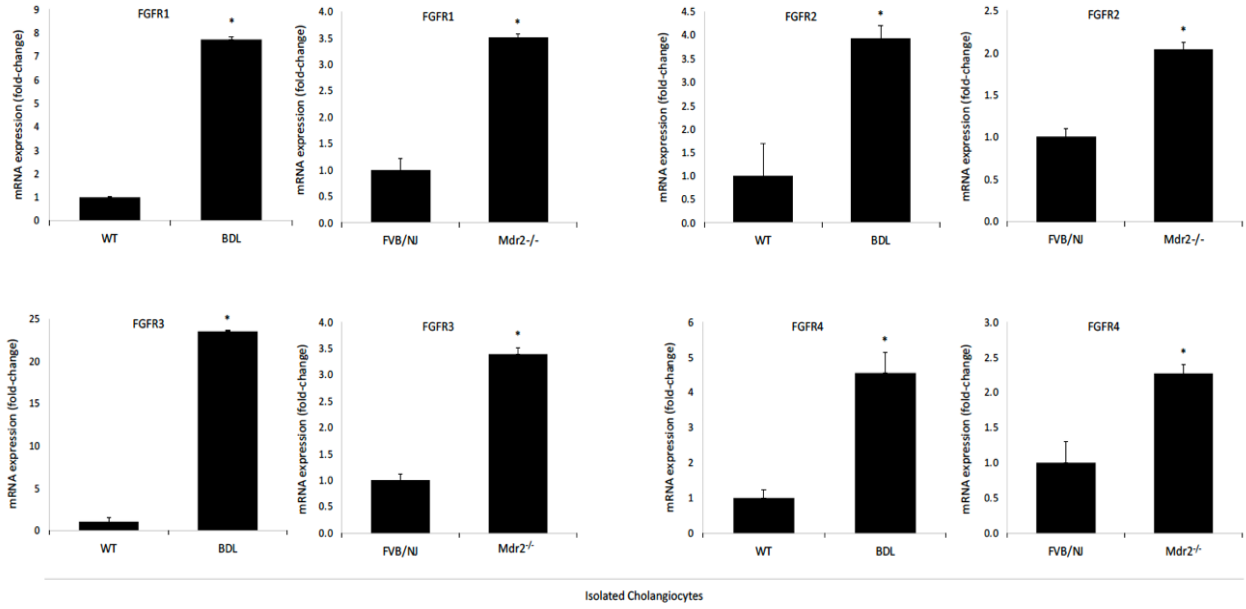

Figure 3: BDL and Mdr2$^{-/-}$ mice have increased *FGFR 1-4* gene expression compared to controls via *q*PCR in isolated cholangiocytes

There was enhanced mRNA expression of *FGFR1-4* in cholangiocytes from both BDL and Mdr2$^{-/-}$ mice compared to control mice. Data are mean ± SEM of 4 *q*PCR reactions from 3 cumulative preparations of isolated cholangiocytes from 9 mice. *p<0.05 vs. C57BL/6 or FVB/NJ mice.

FGF1 immunoreactivity, serum levels, and mRNA expression from isolated cholangiocytes

By immunofluorescence, FGF1 immunoreactivity was evaluated in total liver OCT sections from FVB controls and Mdr2$^{-/-}$ animals, along with AZD4547 treatment groups. These images clearly show increased immunoreactivity of FGF1 colocalized with the CK19 positive bile ducts (in blue) that is absent in the hepatic stellate cells (in green). Treatment with AZD4547 significantly reduces the immunoreactivity in both the FVB and Mdr2 treatment groups when compared to controls (Figure 4). FGF1 serum levels were evaluated in FVB and Mdr2$^{-/-}$ mice in addition to AZD4547 treatment groups. There was a significant increase in levels from Mdr2$^{-/-}$ animals compared to controls. These levels were dramatically reduced with AZD4547 treatment (Figure 5). Genetically modified Mdr2 animals have increased mRNA expression of *FGF1* when compared to FVB controls, which was brought to below normal values following treatment with FGFR antagonist AZD4547. No significant changes were noted in either serum or mRNA in FVB/NJ mice treated with AZD4547 (Figure 5).

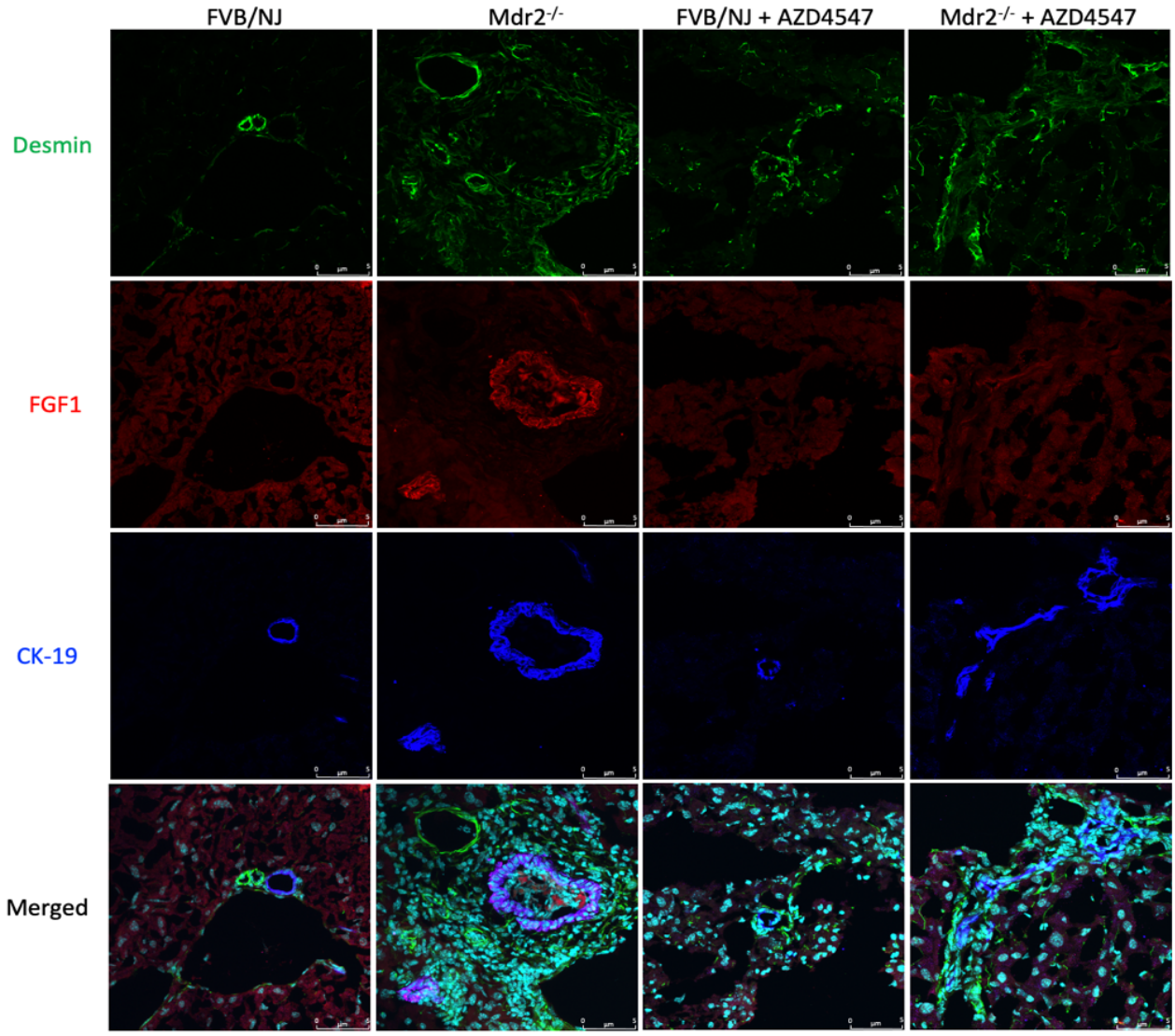

Figure 4: Evaluation of FGF1 immunoreactivity in OCT liver sections from FVB, Mdr2$^{-/-}$, and treatment groups

There was enhanced immunoreactivity for FGF1 (red) in cholangiocytes in liver sections co-stained with CK-19 (blue) from Mdr2$^{-/-}$ mice, immunoreactivity that was decreased by treatment with AZD4547. No immunoreactivity for FGF1 was observed for HSCs in liver sections co-stained with desmin (green). Scale bar = 5 μm.

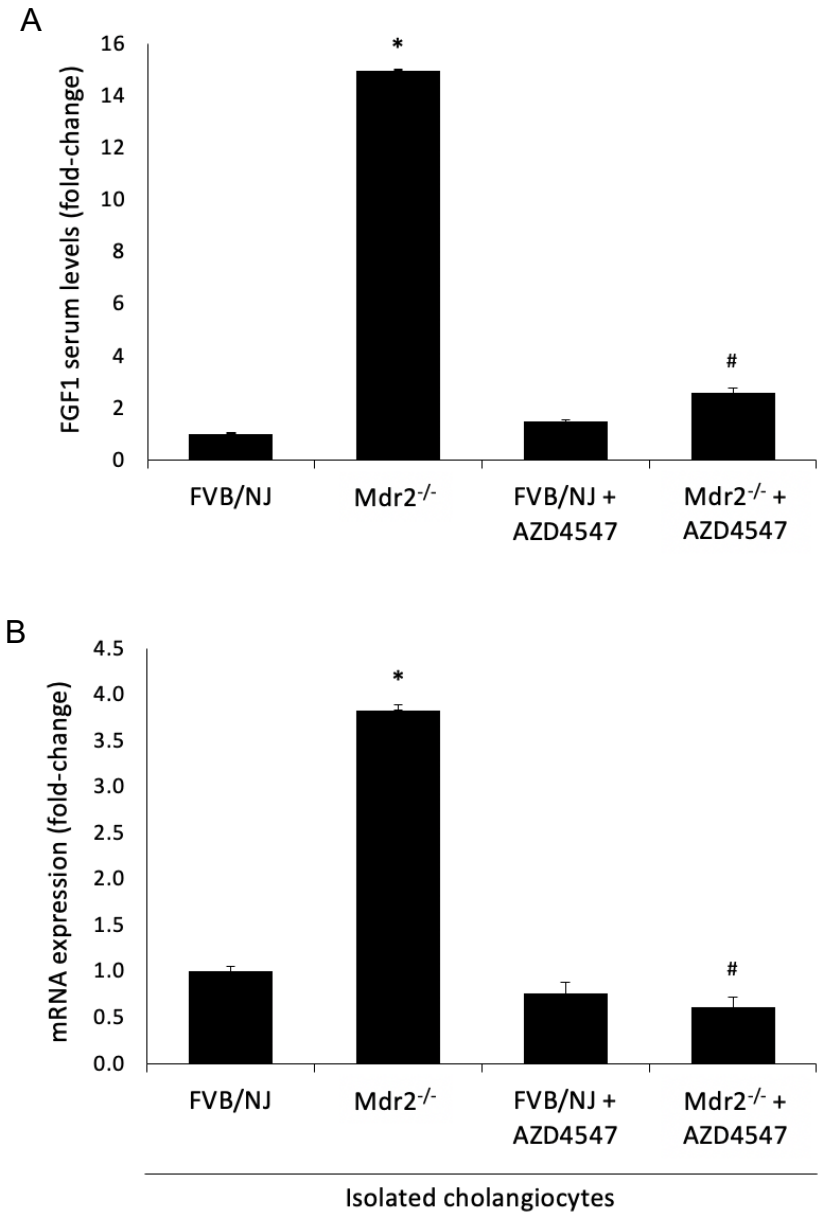

Figure 5: FGF1 serum levels and mRNA expression increased in Mdr2-/- mice, decreased by treatment with AZD4547

There were increased FGF1 serum levels **[A]** and upregulated gene expression **[B]** in Mdr2$^{-/-}$ mice compared to controls. Data are mean ± SEM of 3 experiments from 9 animals for FGF1 serum levels. Data are mean ± SEM of 4 *q*PCR reactions from 3 cumulative preparations of isolated cholangiocytes from 9 mice. *p<0.05 vs. C57BL/6 or FVB/NJ mice.

Changes in IBDM and biliary proliferation

As denoted by the blue arrows and in agreement with previous studies, [96,87] there was enhanced IBDM in BDL compared to WT mice (Figure 6), which was further exacerbated by rhFGF1 compared to control animals. WT mice also had increased IBDM following treatment with rhFGF1 when compared to control which was significantly reduced by receptor antagonist AZD4547 in both BDL and WT groups (Figure 6). IBDM was markedly higher in the Mdr2$^{-/-}$ compared to FVB/NJ mice (blue arrows), which was reduced in Mdr2$^{-/-}$ mice treated with AZD4547 or anti-FGF1 monoclonal antibody (Figure 7). To confirm these findings, the mRNA expression of *Ki67* and *PCNA* was evaluated via *q*PCR. Ki67 is a nuclear protein produced by actively dividing cells. Figure 8 shows isolated cholangiocytes from the Mdr2 knockout animals significantly overexpress *Ki67* when compared to FVB controls, levels that are reduced by more than half in control and injury groups by treatment with AZD4547. PCNA, or proliferating cell nuclear antigen, is a highly conserved nuclear protein found in replicating cells that serves as cofactor for DNA polymerase delta. As with *Ki67*, there was increased *PCNA* gene expression in Mdr2$^{-/-}$ mice compared to FVB, that were significantly reduced to more than half in both the FVB + treatment group and Mdr2$^{-/-}$ + treatment group. (Figure 8).

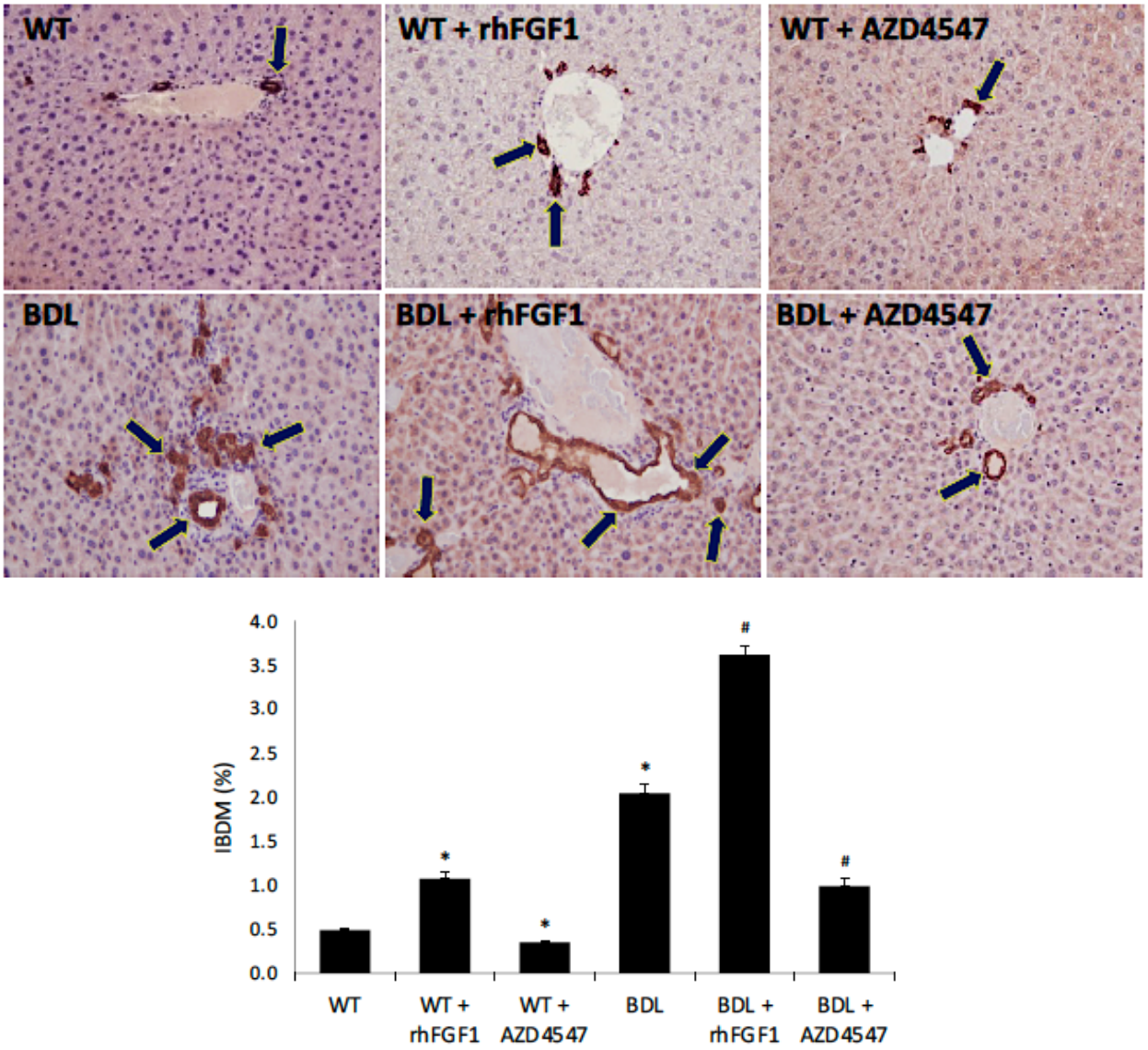

Figure 6: rhFGF1 increases intrahepatic bile duct mass in WT and BDL animals which is lowered by AZD4547 in BDL and WT groups

There was increased IBDM in BDL mice compared to C57BL/6 (WT) mice and in both C57BL/6 and BDL mice treated with recombinant human FGF1 compared to control animals, increases that were significantly reduced by AZD4547. Data are mean ± SEM of 9 total liver sections, 10 fields of view, original magnification, 20x. *p<0.05 vs. C57BL/6; #p<0.05 vs. BDL. Black arrows outlined in yellow indicate CK-19-positive bile ducts.

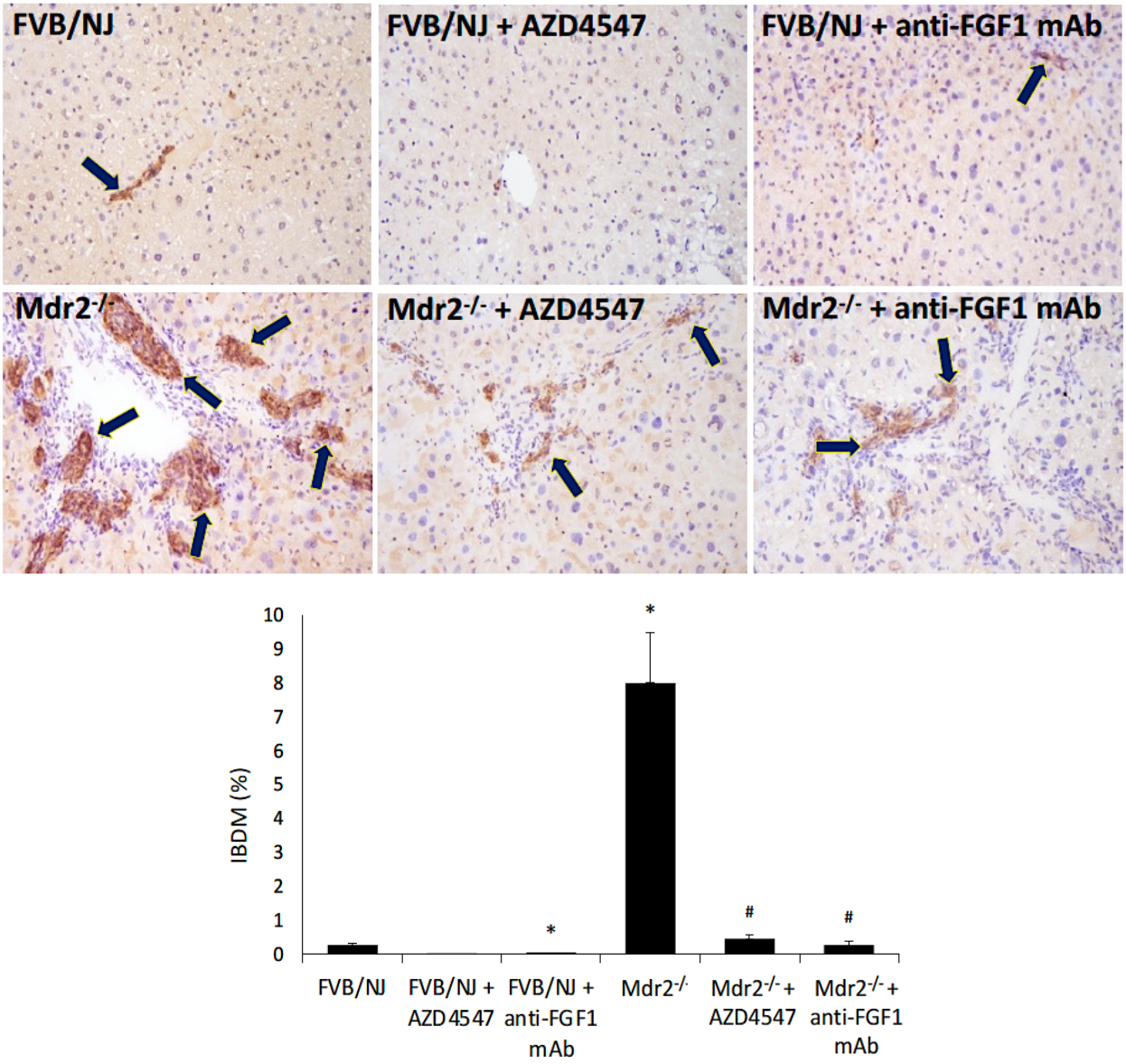

Figure 7: FGFR antagonist and FGF1 antibody decrease IBDM in Mdr2$^{-/-}$ mice in FFPE liver sections

IBDM was higher in Mdr2$^{-/-}$ mice compared to FVB/NJ mice, which was reduced by AZD4547 or anti-FGF1 monoclonal antibody. Data are mean ± SEM of 9 total liver sections, 10 fields of view, original magnification, 20x. *p<0.05 vs. FVB/NJ mice; #p<0.05 vs. Mdr2$^{-/-}$ mice. Yellow arrows indicate CK-19 positive bile ducts.

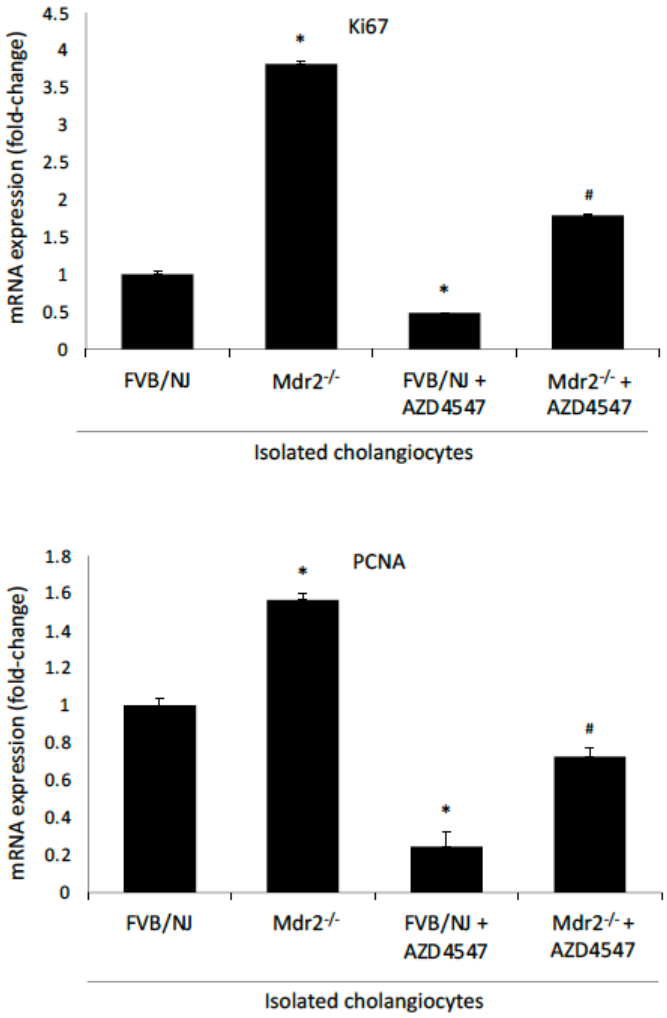

Figure 8: AZD4547 reduces gene expression in proliferation markers in Mdr2$^{-/-}$ and FVB treated animals compared to controls

There was increased expression of *Ki67* and *PCNA* mRNA in isolated cholangiocytes from Mdr2$^{-/-}$ mice compared to control mice that was significantly decreased in mice treated with AZD4547. Data are mean ± SEM of 4 *q*PCR reactions from 3 preparations of isolated cholangiocytes from 9 animals. *p<0.05 vs. FVB/NJ mice; #p<0.05 vs. Mdr2$^{-/-}$ mice.

Evaluation of liver fibrosis via Sirius red and *q*PCR

As noted previously, resident hepatic stellate cells, upon leaving their quiescent state, enter an activated state in which they begin to produce and deposit collagen within the parenchyma. As seen in Figure 1, there was an increase in desmin^{+} hepatic stellate cells in BDL injured animals compared to WT control. Therefore, an increase in collagen in liver sections from BDL animals would be expected. Compared to the WT controls, BDL animals have significantly increased levels of collagen deposition, as shown by Sirius red staining (Figure 9). Administration of recombinant human FGF1 further increased collagen deposition, in both the WT and BDL animal groups. Treatment with AZD4547 brought significant reductions in both groups when compared to controls (Figure 9).

Figure 10 evaluated AZD4547 treatment in our chronic mouse model. The FVB animal groups show little to no collagen deposition as seen in the Sirius red staining and denoted by the graphical representation. However, Mdr2$^{-/-}$ knockout animals have large amounts of collagen deposition as demonstrated by the vibrant red staining in the bottom left panel (Figure 10). Treatment with AZD4547 significantly reduced the amount of collagen present within the tissue, with even further reduction in the anti-FGF1 monoclonal antibody treatment group (Figure 10).

To confirm the Sirius red images, we next looked at the expression of various fibrosis markers in total liver. Flash frozen liver chunks were homogenized, and total RNA was isolated. Various fibrosis genes were measured such as alpha smooth muscle actin (*αSMA*), collagen 1 alpha 1 (*Col1α1*), and transforming growth factor beta 1, or *TGF-β1*. αSMA has been shown to be associated with the TGF-β pathway and

enhances the contractility of hepatic stellate cells. In Figure 11 there was a significant increase in *αSMA* in Mdr2 knockout animals compared to FVB, treatment with FGF receptor antagonist brough these levels back to control.

The extra cellular matrix of an organ is a complex network of various components such as collagen, elastin, fibronectin, and laminins etc. The major component is collagen, typically type I which is made up of two chains, collagen type I alpha I, and collagen type I alpha 2. In total liver we looked at the expression of *Col1α1*, and as with the *αSMA*, there was a dramatic increase in Mdr2$^{-/-}$ animals compared to controls, which was decreased by more than half with AZD4547 treatment. Next was consideration of *TGF-β1*. TGF-β1 has been shown to participate in the fibrogenic pathway through the activation of col1α1. As with *col1α1* expression, there was a significant increase in *TGF-β1* in the Mdr2$^{-/-}$ animals compared to FVB, that was decreased in the AZD4547 group (Figure 11).

Elevated TGF-β1 serum levels were noted in the Mdr2$^{-/-}$ knockout animals compared to controls. Like the PCR results, Mdr2$^{-/-}$ animals treated with AZD4547 had decreased TGF-β1 levels, along with animals in the anti-FGF1 mAb group (Figure 11).

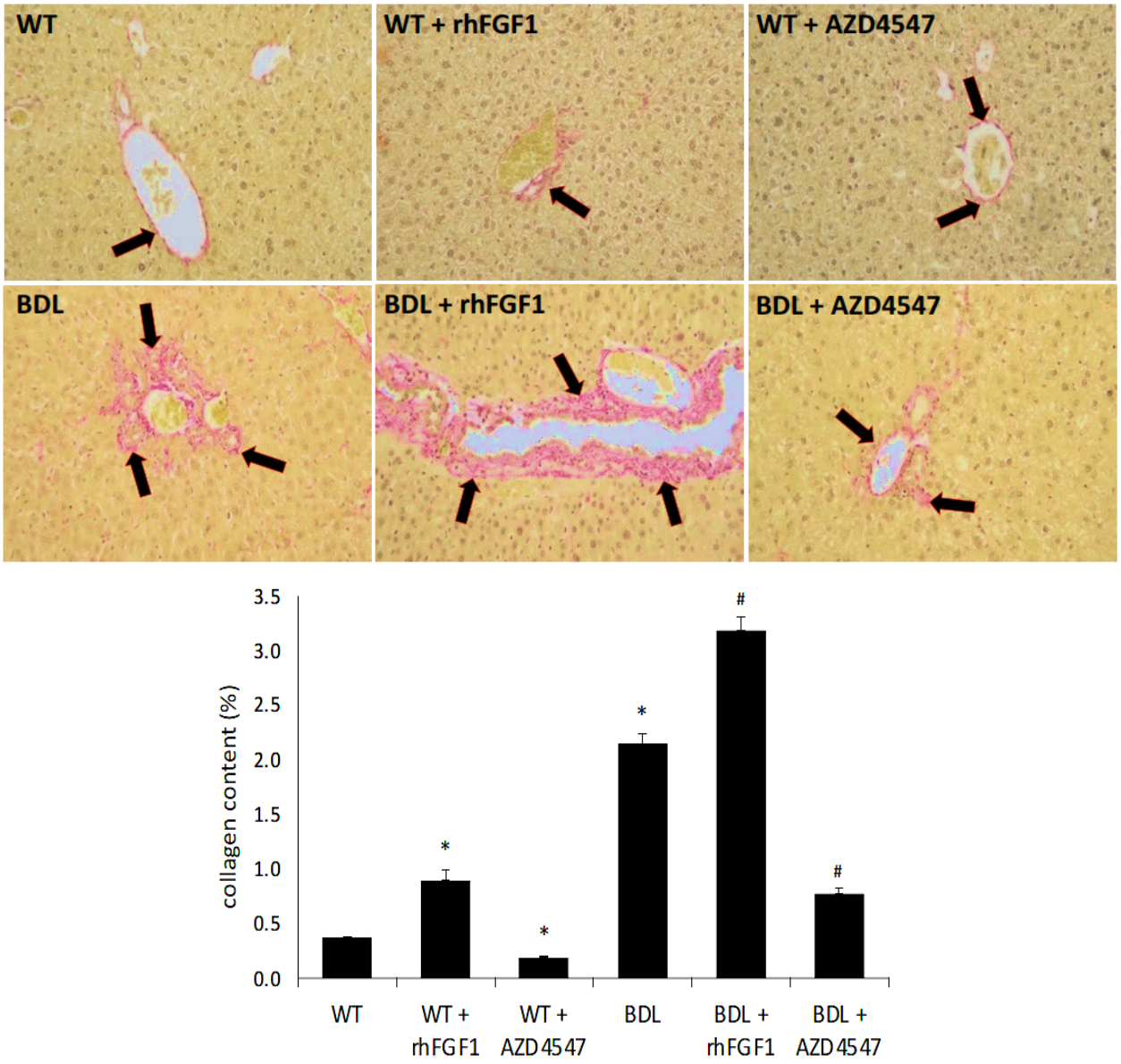

Figure 9: rhFGF1 increases collagen deposition in FFPE liver sections from BDL and WT mice which is reduced by FGFR antagonist

There was enhanced collagen deposition in BDL compared to C57BL/6 mice, as well as C57BL/6 and BDL mice treated with recombinant human FGF1 compared to control animals, increases that were significantly reduced by treatment with AZD4547. Data are mean ± SEM of 6 total liver sections, 10 fields of view from 9 animals, original magnification, 20x. *$p<0.05$ vs. C57BL/6 mice; #$p<0.05$ vs. BDL mice. Red arrows indicate collagen deposition around bile ducts.

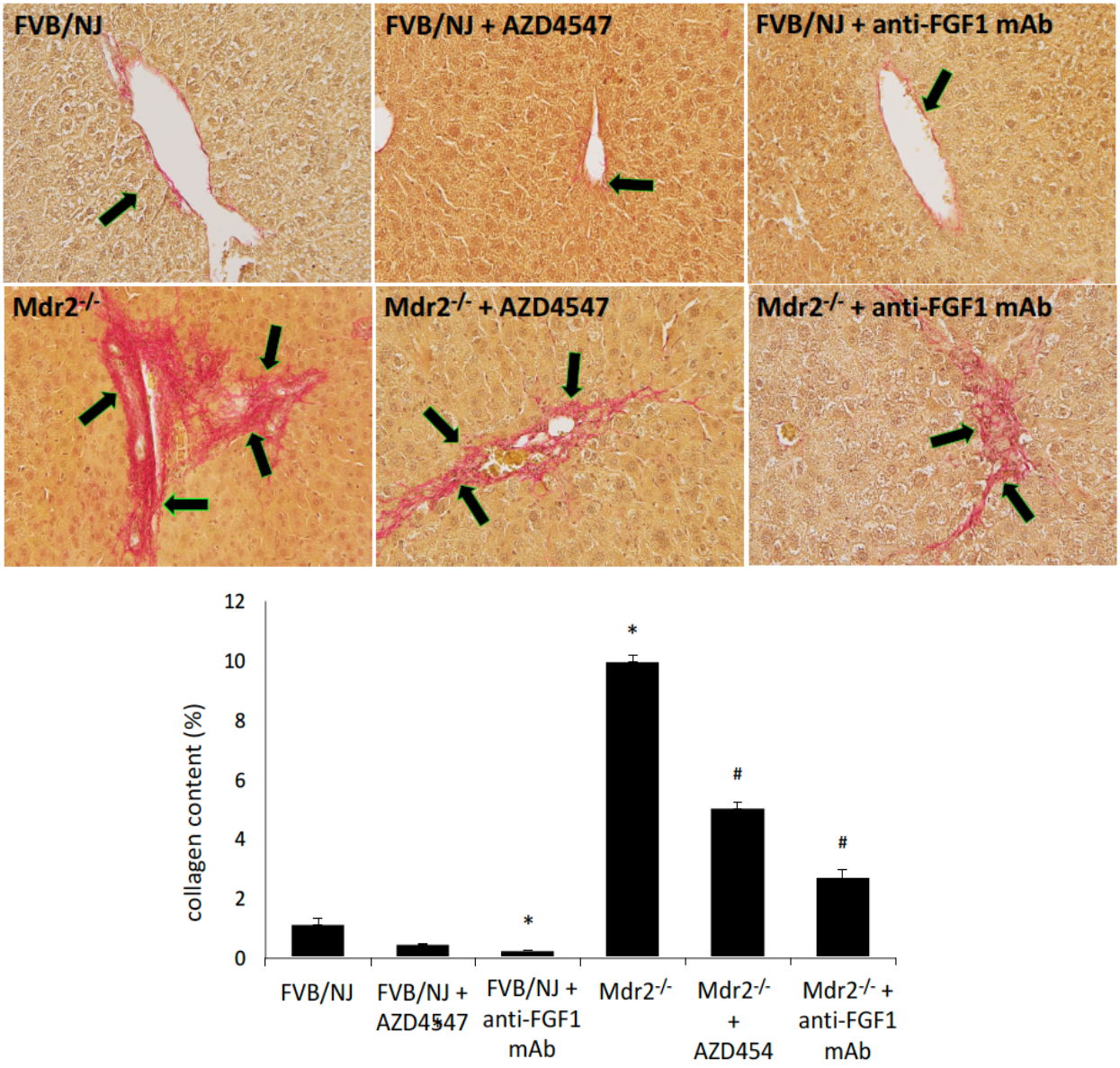

Figure 10: AZD4547 and anti-FGF1 mAb reduce collagen deposition in FVB and Mdr2$^{-/-}$ mice compared to controls

In Mdr2$^{-/-}$ mice there was enhanced liver fibrosis compared to FVB/NJ mice, which was reduced by treatment with AZD4547 or anti-FGF1 monoclonal antibody. Data are mean ± SEM of 6 total liver sections, 10 fields of view from 9 animals, original magnification, 20x. *p<0.05 vs. FVB/NJ mice; #p<0.05 vs. Mdr2$^{-/-}$ mice. Red arrows indicate collagen deposition around bile ducts.

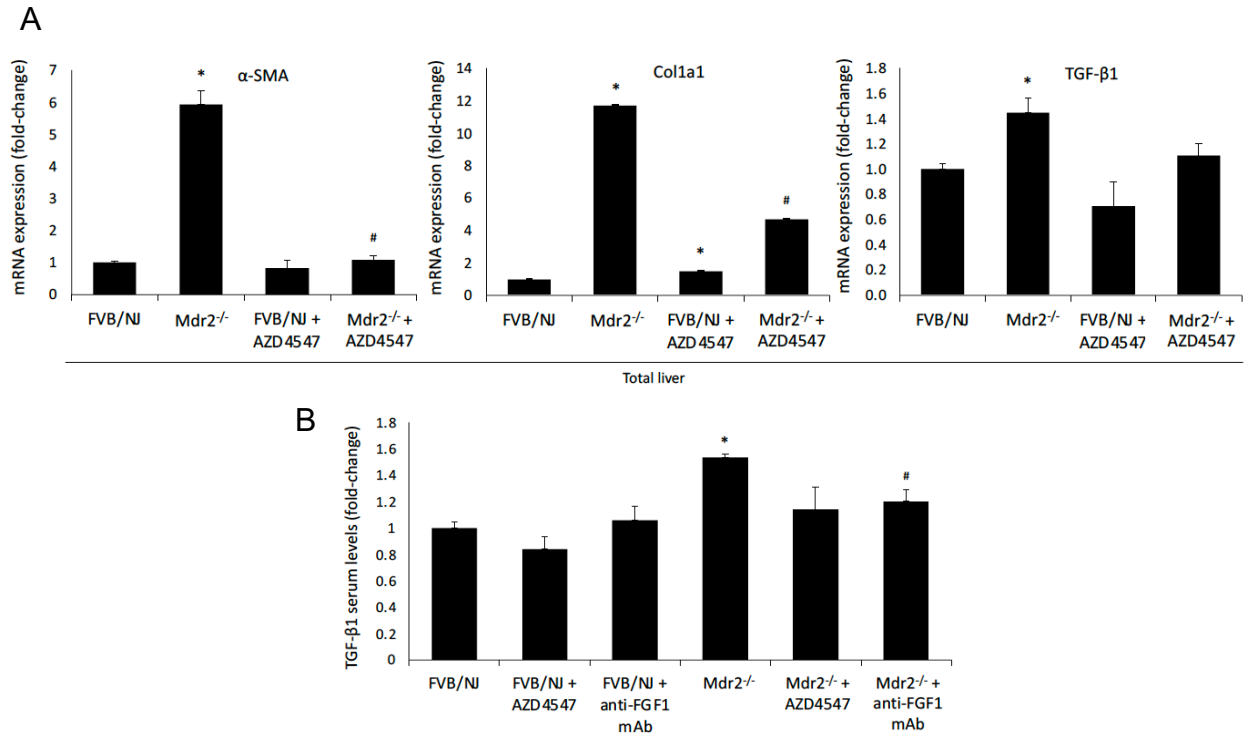

Figure 11: AZD4547 decreases gene expression and serum protein of fibrosis markers via *q*PCR or ELISA in isolated cholangiocytes or supernatants from FVB, Mdr2$^{-/-}$, and treatment groups

There was increased mRNA expression **[A]** of *α-SMA*, *Col1a1*, and *TGF-β1* (in total liver samples) and TGF-β1 serum levels [B] in Mdr2$^{-/-}$ mice compared to FVB/NJ mice, increases that were significantly decreased by AZD4547 or anti-FGF1 monoclonal antibody compared to untreated Mdr2$^{-/-}$ mice. Data are mean ± SEM of 4 *q*PCR reactions from 3 cumulative preparations of isolated cholangiocytes from 9 animals. Data are mean ± SEM of 3 experiments from 9 animals for TGF-β1 serum levels. *p<0.05 vs. FVB/NJ mice; #p<0.05 vs. Mdr2$^{-/-}$ mice.

IHC and *q*PCR evaluation of inflammation

F4/80 is an antibody used to identify macrophage populations within total liver sections. Via IHC, there was noted to be an increase of $F4/80^+$ cells in WT animals treated with recombinant human FGF1 when compared to WT, along with a significant reduction in the WT + AZD4547 group (Figure 12). There is also a significant increase in the BDL group when compared to the WT animals, which is further increased by treatment with rhFGF1. Not only is there a greater population of macrophages throughout the tissue, in the BDL and BDL + recombinant human FGF1 there is increased staining present around the bile ducts. AZD4547 significantly reduces the macrophage presence when compared to WT controls.

Similarly, in $Mdr2^{-/-}$ mice, there was a significant influx of macrophage presence (as denoted by dark blue arrows) compared to FVB controls Both AZD4547 and anti-FGF1 monoclonal antibody significantly decreased murine macrophage populations (Figure 13). Percent $F4/80^+$ cells were determined using the number of positive pixels/total pixels x 100. Visio Pharm set the threshold based on application algorithms and these remained consistent for each set of images.

By *q*PCR the gene expression of interleukin 6 (*IL-6*) was evaluated. The production of IL-6 is an immediate immune response to tissue injury or infection, and while this plays a critical role in an organism's immune defense, ongoing synthesis is detrimental in cases of chronic inflammation. *IL-6* expression in isolated cholangiocytes from the $Mdr2^{-/-}$ animals was significantly increased, and treatment with AZD4547 lowered expression in both the FVB and $Mdr2^{-/-}$ treatment groups when compared to controls (Figure 14). Next was the evaluation of interleukin-1β expression (*IL-1β*), followed by IL-1β serum levels.

Like IL-6, IL-1β is a pro-inflammatory cytokine necessary for an organism's defense against infection and injury. Left unchecked, IL-1β exacerbates tissue damage during chronic disease. In both serum and isolated cholangiocytes, $Mdr2^{-/-}$ animals had increased IL-1β, and in both cases treatment with AZD4547 brought it down to below FVB control levels (Figure 14).

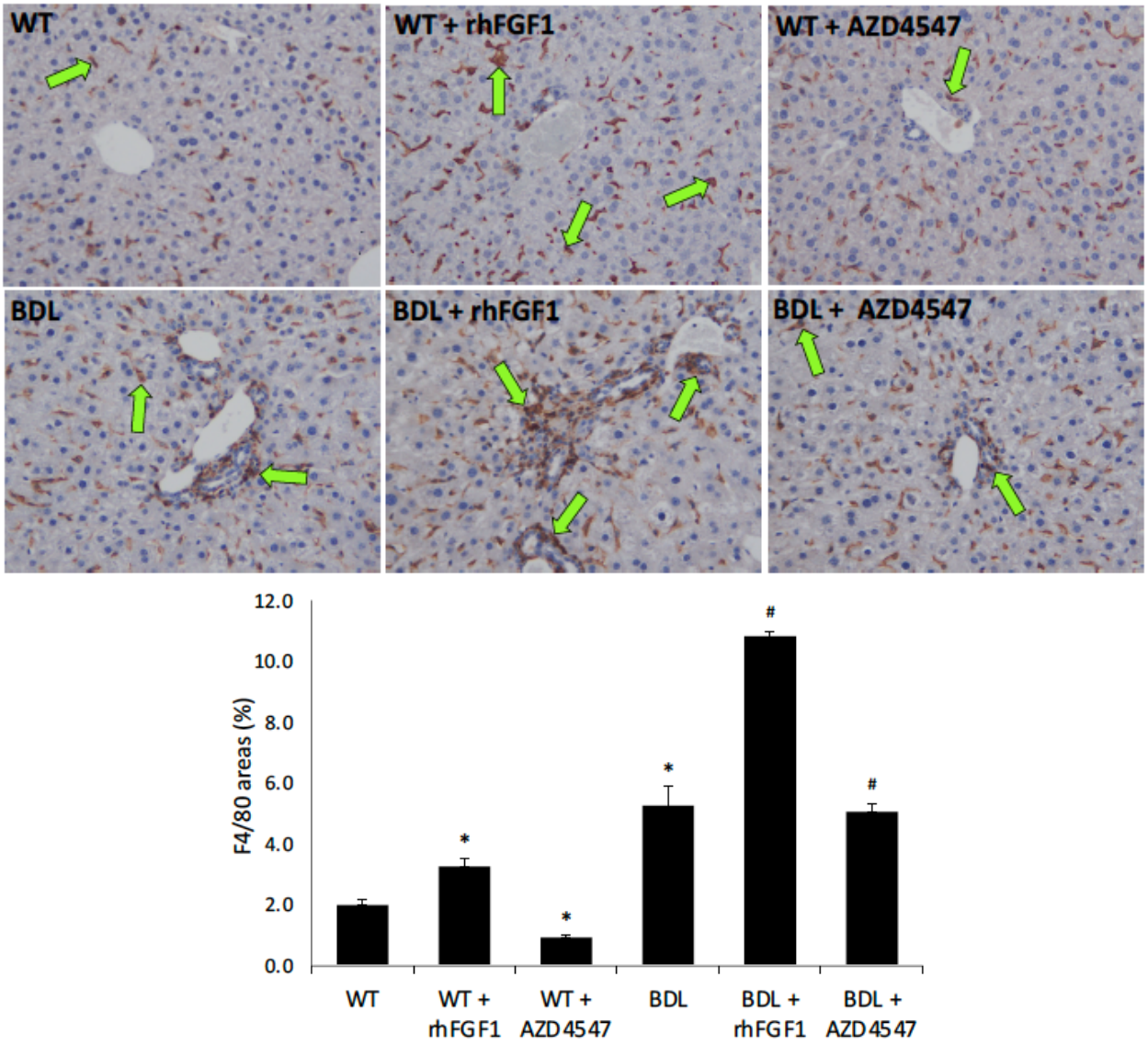

Figure 12: rhFGF1 increased murine macrophages in WT and BDL animals; FGFR antagonist decreases populations in WT and BDL

There was increased F4/80 immunoreactivity in liver sections from BDL compared to WT mice, which was ameliorated by treatment with AZD4547. F4/80 immunoreactivity increased in both C57BL/6 and BDL mice treated with the rhFGF1. Data are mean ± SEM of 6 total liver sections, 10 fields of view, from 9 animals, original magnification, 20x. *p<0.05 vs. C57/BL6 mice; #p<0.05 vs. BDL mice. Green arrows indicate F4/80-positive cells.

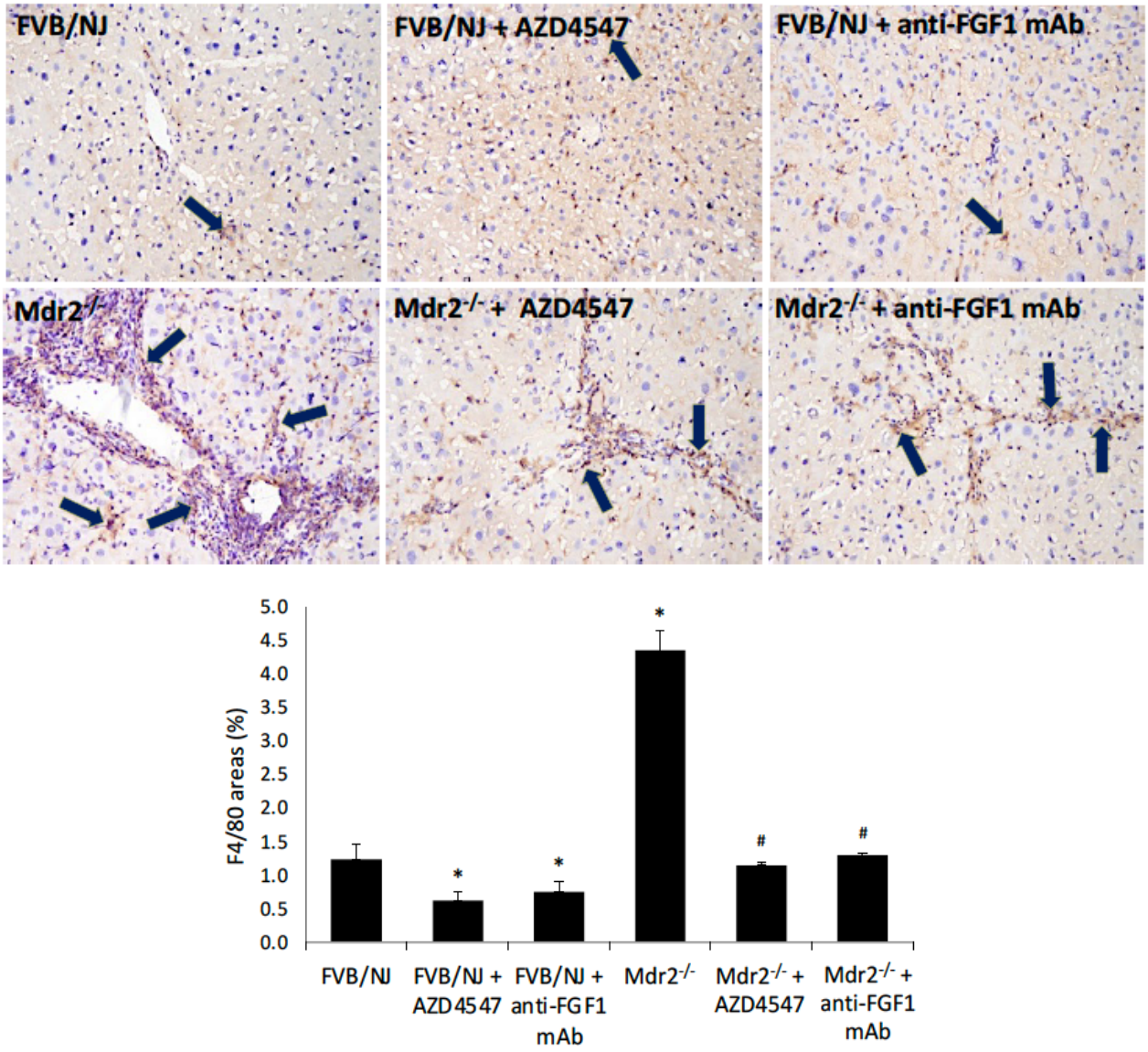

Figure 13: Anti-FGF1 mAb and FGFR antagonist decreases F4/80+ cells in FVB and Mdr2-/- animals compared to controls

There was increased F4/80 immunoreactivity in the $Mdr2^{-/-}$ compared to FVB/NJ mice, which was reduced by treatment with either AZD4547 or anti-FGF1 mAb. Data are mean ± SEM of 6 total liver sections, 10 fields of view from 9 animals, original magnification, 20x. *p<0.05 vs. FVB/NJ mice; #p<0.05 vs. $Mdr2^{-/-}$ mice. Navy blue arrows indicate F4/80 positive cells.

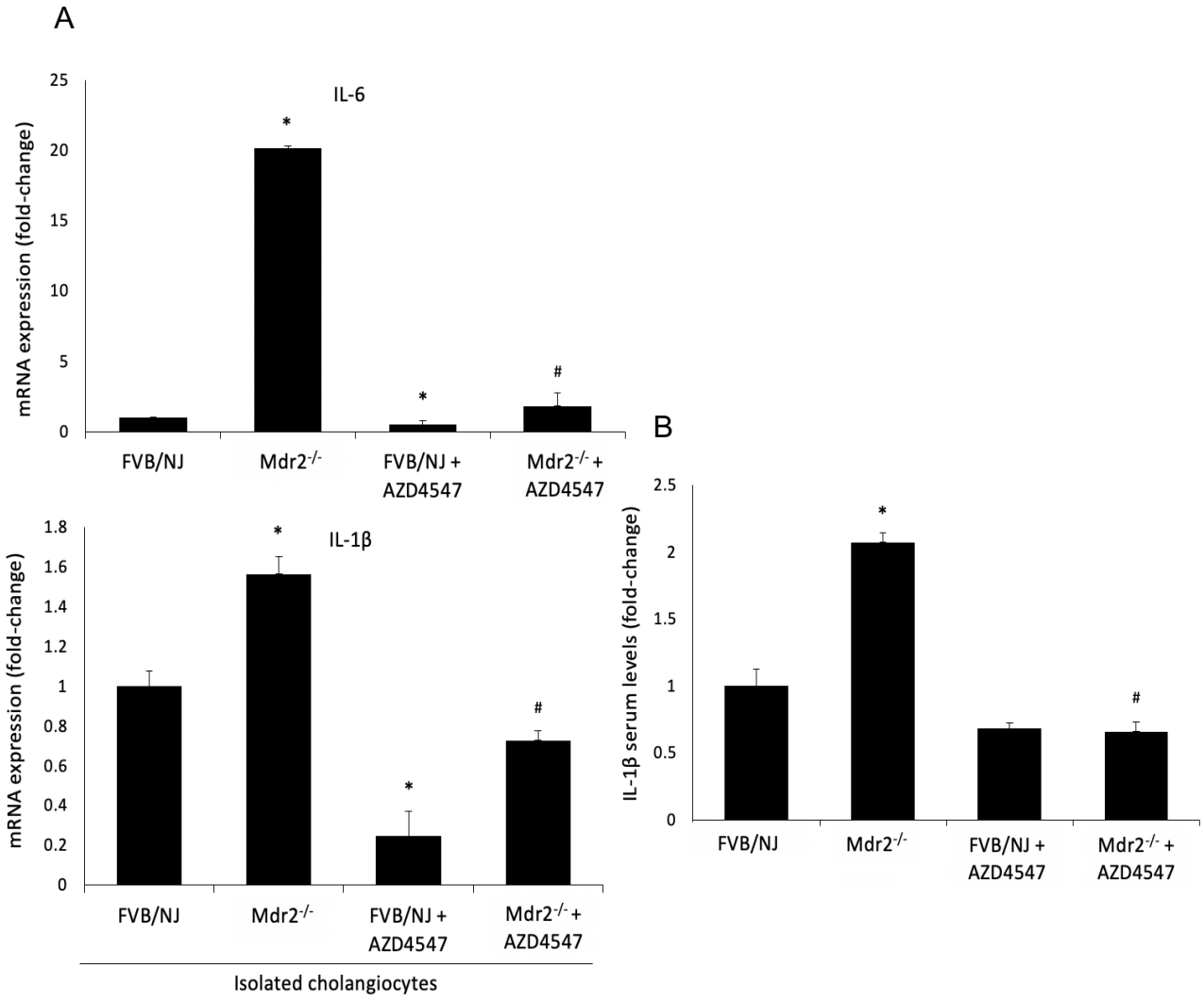

Figure 14: By qPCR and ELISA there was a decrease in inflammatory markers and serum protein in Mdr2-/- animals treated with AZD4547

[A] The mRNA expression of *IL-6* and *IL-1β* was higher in cholangiocytes from the Mdr2$^{-/-}$ compared to FVB/NJ mice but decreased in cholangiocytes from Mdr2$^{-/-}$ mice treated with AZD4547. Data are mean ± SEM of 4 *q*PCR reactions from 3 cumulative preparations of cholangiocytes from 9 animals. *p<0.05 vs. Mdr2$^{-/-}$ mice. **[B]** Mdr2$^{-/-}$ mice had increased serum IL-1β levels compared to control mice, which were decreased in Mdr2$^{-/-}$ mice treated with AZD4547 compared to vehicle-treated Mdr2$^{-/-}$ mice. Serum levels were measured in 3 samples from 9 different animals. *p<0.05 vs. FVB/NJ mice; #p<0.05 vs. Mdr2$^{-/-}$ mice.

Evaluation of senescence via total liver SA-β-Gal and *q*PCR in isolated cholangiocytes

In OCT liver sections from FVB, Mdr2$^{-/-}$, and AZD4547 treatment groups, we looked for the presence of senescence associated β galactosidase, or SA-β-Gal. β galactosidase is a lysosomal enzyme that can cleave the glycosidic bond in X-gal, forming galactose and an oxidation product resulting in a bright blue color. Figure 16 shows an increase in blue product, indicating the increased presence of SA-β-Gal in the Mdr2$^{-/-}$ liver sections when compared to the FVB control. This is significantly reduced in the FVB + AZD4547, which has no detectable blue staining, and the Mdr2$^{-/-}$ + AZD4547 treatment group, where very little color is detected in the tissue and as seen in the graphical representation of the data (Figure 15). Despite the idea that senescence is an arrest of the cell cycle, this data does not dispute our previous findings of increased proliferation of the bile ducts. It is clearly seen in the Mdr2$^{-/-}$ section, that only a portion of the cholangiocytes express this senescence marker. The surrounding cells and other ducts remain pink, indicating they are in a functional proliferative state. Furthermore, while these cells may be arrested, they are continuing to be metabolically functional, and have been shown to have increased secretions of inflammatory cytokines such as IL-6 and IL-1.

In OCT liver sections by immunofluorescence, the immunoreactivity of p16 was determined. There is an increase of p16 immunoreactivity (red) in and around the cells of the bile ducts (blue) in the Mdr2$^{-/-}$ knockout animals compared to FVB controls. This was reduced by treatment with AZD4547 in both groups (Figure 16).

The gene expression of *p16*, *p21*, and *p53* was measured in isolated cholangiocytes via *q*PCR. p16 is a major contributor to cell cycle regulation through the

binding of cyclin-dependent kinase 4/6 which inhibits a necessary protein complex from forming that phosphorylates pocket protein Rb. In absence of phosphorylation, Rb proteins bind to E2F1, preventing this transcription factor from promoting gene expression of the necessary genes involved in cell cycle S-phase entry. There was an upregulation of *p16* in the Mdr2$^{-/-}$ animals, with a significant decrease in AZD4547 treatment group (Figure 17). The expression of *p21* was also considered. p21 regulates cellular proliferation through its direct interaction with cyclin dependent kinases, and its ability to associate with PCNA and inhibit its function, thereby stopping DNA replication. As with *p16*, there was increased levels of *p21* in our Mdr2$^{-/-}$ knockout animals, levels which were brought within FVB control level by treatment with AZD4547 (Figure 17).

The expression level of *p53* was also assessed. p53, is a well-known tumor suppressor gene, and has been previously established as a transcription factor by binding to promoter regions or interacting with coactivators of target genes. An increase in p53 leads to the downstream transcriptional activation of p21, which pushes the cell to arrest, protecting the cell from further DNA damage. As with *p21*, there is a similar expression pattern of *p53* increase in the isolated cholangiocytes from the Mdr2$^{-/-}$ knockout animals compared to FVB controls, followed by significant decreases in the AZD4547 treatment groups (Figure 17).

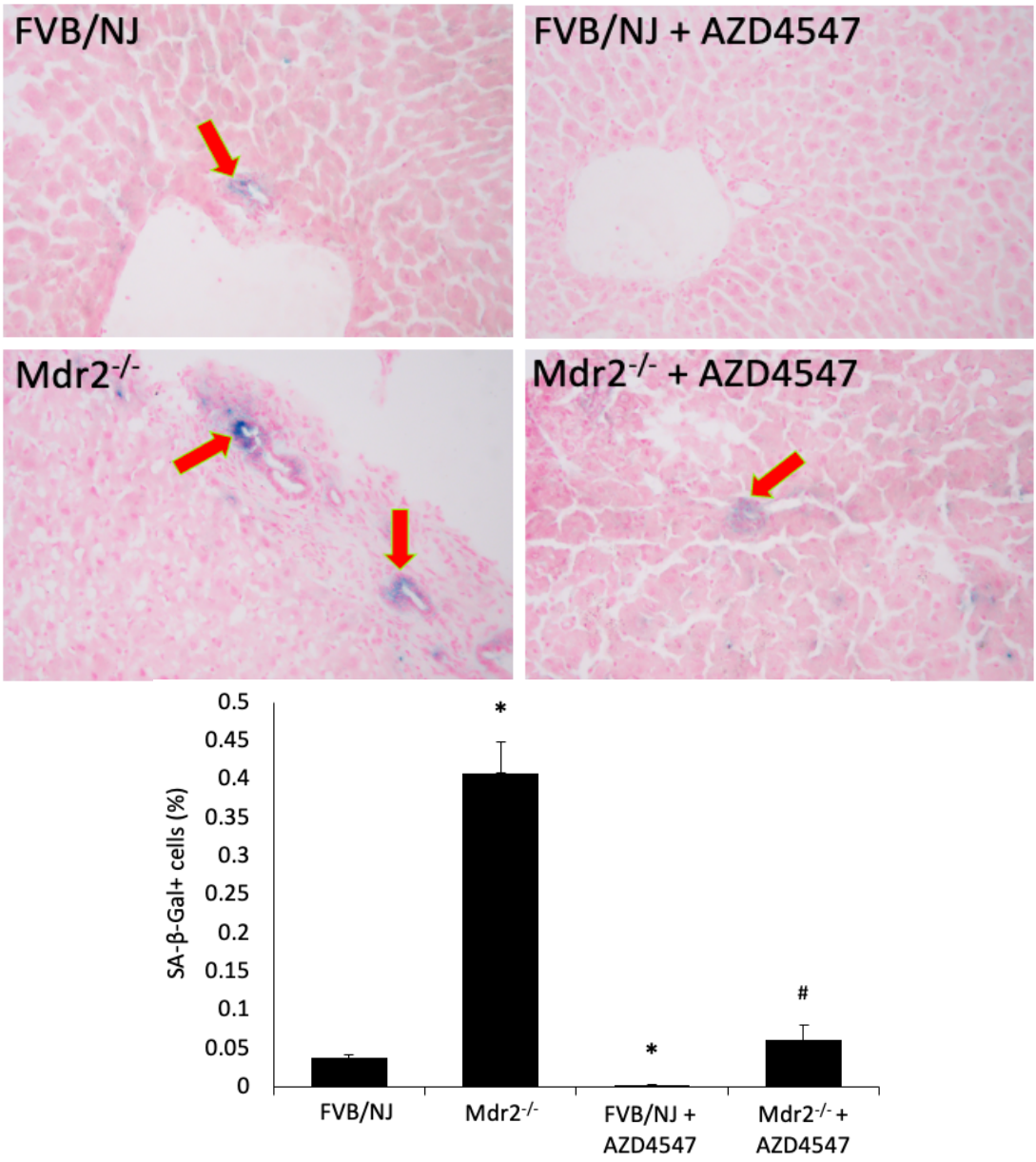

Figure 15: AZD4547 treatment reduces SA-B-Gal+ cells in total liver OCT sections

By SA-β-Gal staining in liver sections, there was enhanced biliary senescence in Mdr2$^{-/-}$ compared to FVB/NJ mice, which was decreased by treatment with AZD4547. Data are mean ± SEM of 4 total liver sections, 6 fields of view, original magnification 20x. *p<0.05 vs. FVB/NJ mice; #p<0.05 vs. Mdr2$^{-/-}$ mice.

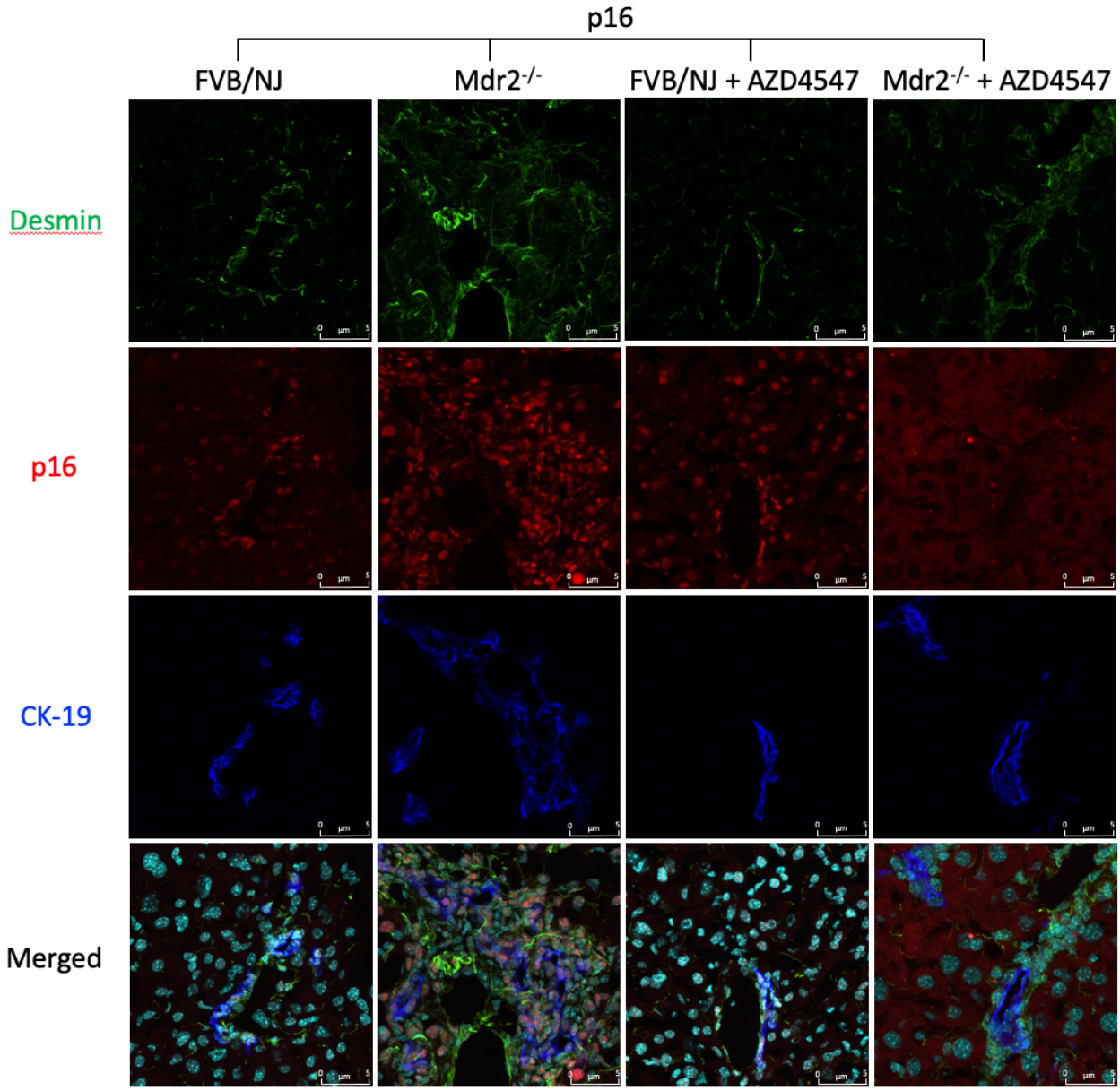

Figure 16: AZD4547 decreases p16 immunoreactivity in FVB and Mdr2-/- mice by immunofluorescence

By immunofluorescence for p16 in liver sections, there was enhanced biliary senescence in Mdr2$^{-/-}$ compared to FVB/NJ mice, which was decreased by treatment with AZD4547. Data are mean ± SEM of 4 total liver sections, 6 fields of view, original magnification 20x. *p<0.05 vs. FVB/NJ mice; #p<0.05 vs. Mdr2$^{-/-}$ mice.

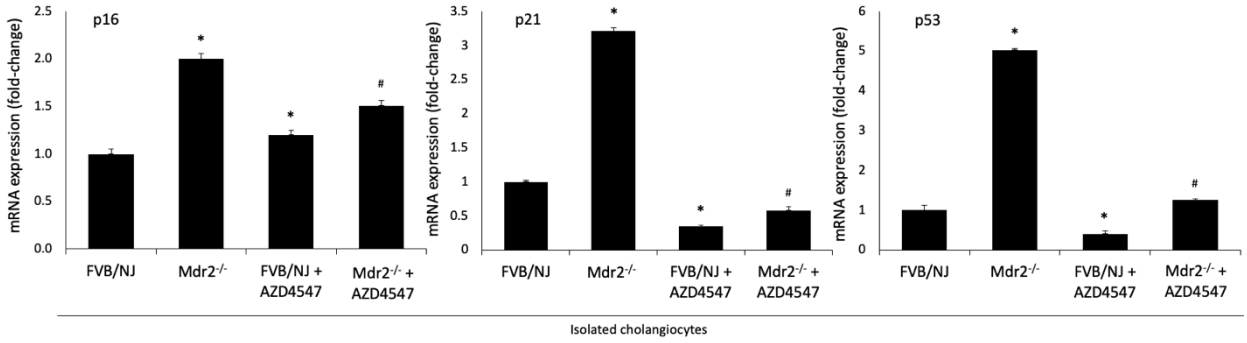

Figure 17: FGFR antagonist reduces gene expression in senescence markers in treatment groups compared to FVB and Mdr2-/- controls

There was increased mRNA expression of *p16*, *p21*, and *p53* in cholangiocytes from Mdr2$^{-/-}$ compared to FVB/NJ mice, which was decreased with AZD4547 treatment. Data are mean ± SEM of 4 *q*PCR reactions from 3 preparations of cholangiocytes from 9 animals. *p<0.05 vs. FVB/NJ mice, #p<0.05 vs Mdr2$^{-/-}$ mice.

CD31 immunoreactivity and genetic markers of angiogenesis

The final hallmark of PSC we examined in our mouse models was angiogenesis. The immunoreactivity of CD31, or platelet endothelial cell adhesion molecule 1 was examined. CD31 is a member of the immunoglobulin superfamily found on platelets, leukocytes, and vascular endothelial cells. While not a marker of angiogenesis, an increase in CD31 demonstrates an increase in vascular endothelial cell presence. Mdr2$^{-/-}$ mice show increased immunoreactivity for CD31 (in red) surrounding the bile ducts (in blue). Administration of AZD4547 decreased the immunoreactivity compared to the control samples (Figure 18A). By *q*PCR there were increased expression levels of CD31 in Mdr2$^{-/-}$ total liver samples, with corresponding decreases in Mdr2$^{-/-}$ + AZD4547 treatment group. Next angiogenin (*ANG*) was measured by *q*PCR in total liver. Angiogenin was discovered in 1985 and was the first tumor-derived protein shown to stimulate growth of new vessels. Angiogenin is a potent angiogenic factor that has been shown to be induced by other growth factors including vascular endothelial growth factor and FGF1. In the Mdr2$^{-/-}$ knockout total liver samples there was a significant increase in *ANG* which treatment with AZD4547 significantly decreases (Figure 18B).

There was a slight increase in angiogenin immunoreactivity in both BDL and Mdr2 liver sections compared to corresponding controls (Figure 19A). In isolated cholangiocytes there was increased expression in both *VEGFA* and *ANG* in the Mdr2$^{-/-}$ group. Both FVB and Mdr2$^{-/-}$ groups treated with the FGFR antagonist had significant decreases compared to controls (Figure 19B).

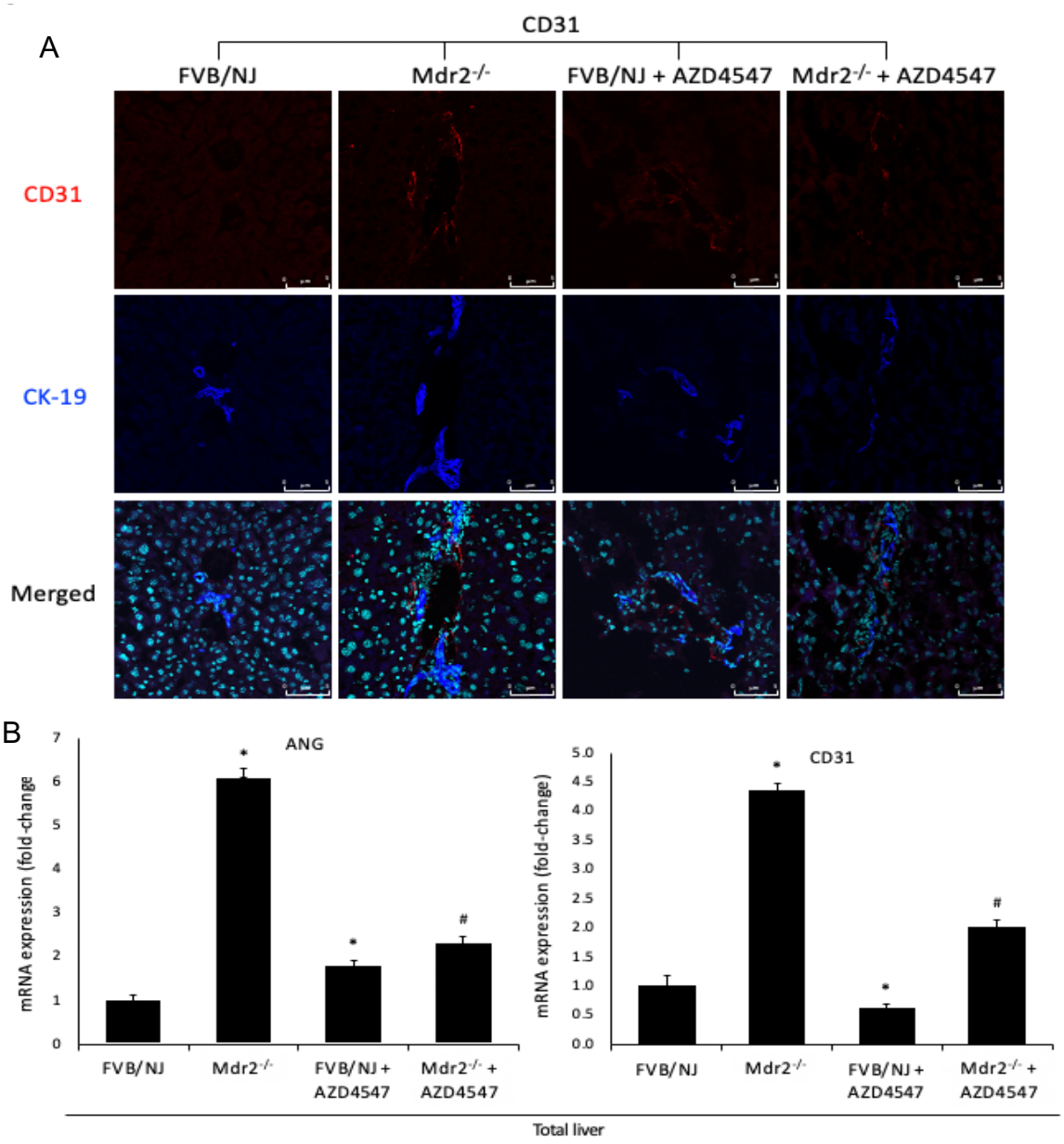

Figure 18: FGFR antagonist reduces vascular endothelial marker immunoreactivity and gene expression of CD31 and angiogenin compared to FVB and Mdr2-/-

[A] Immunoreactivity of CD31 (in liver sections) and **[B]** mRNA expression of *ANG* and *CD31* (in total liver) increased in Mdr2$^{-/-}$ mice compared to the corresponding FVB/NJ mice; parameters that were significantly reduced by AZD4547. Scale bar = 5 μm. **[B]** Data are mean ± SEM of 4 *q*PCR reactions from 3 preparations of isolated cholangiocytes or total liver from 9 animals. *p<0.05 vs. FVB/NJ, #p<0.05 vs Mdr2$^{-/-}$ mice.

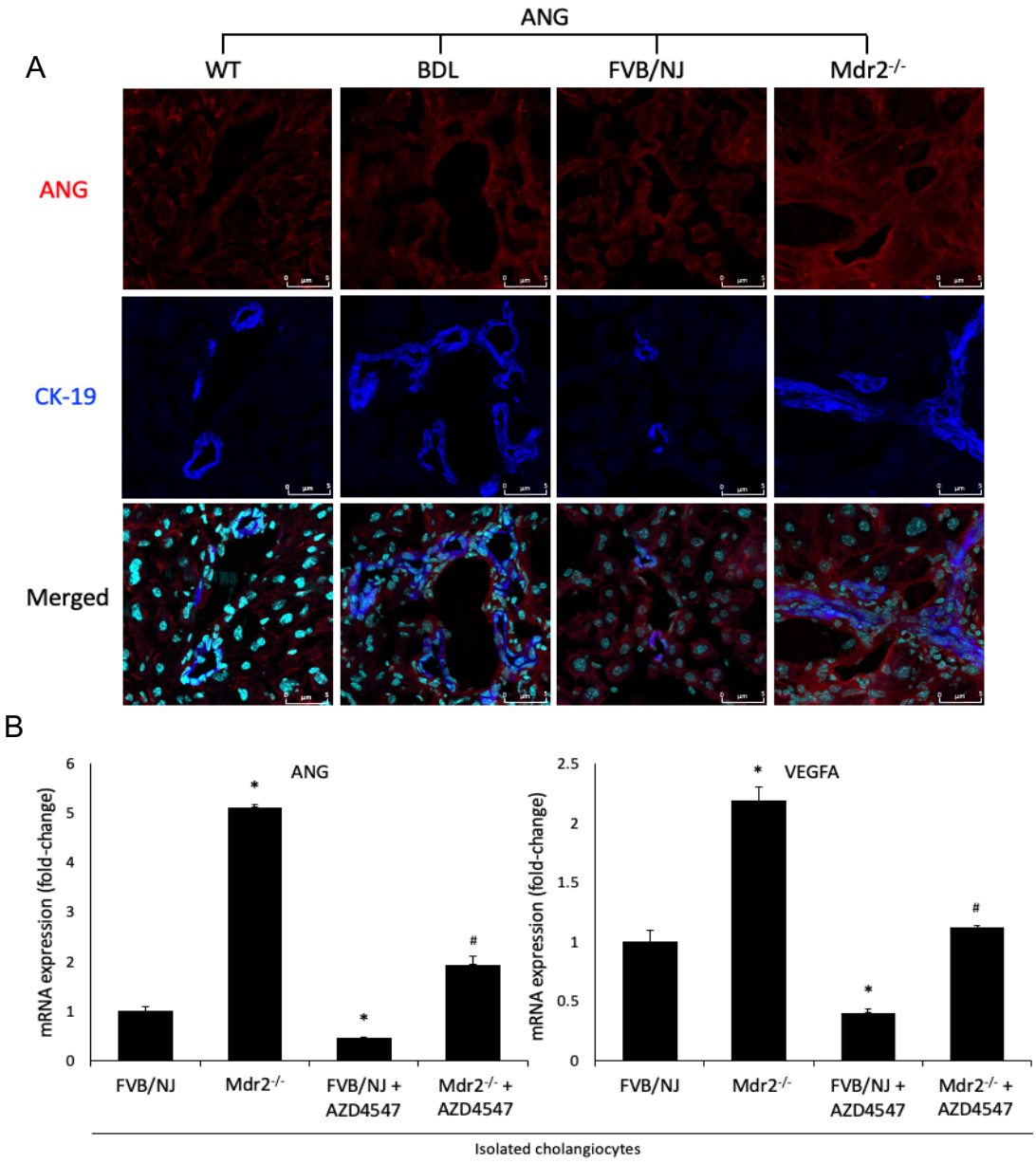

Figure 19: Angiogenin immunoreactivity increases in BDL and Mdr2-/- mice; AZD4547 decreases angiogenesis gene expression in Mdr2-/- treatment groups

[**A-B**] Immunoreactivity of ANG (in liver sections) and mRNA expression of *ANG* and *VEGFA* (in isolated cholangiocytes) increased in Mdr2$^{-/-}$ mice compared to the corresponding FVB/NJ mice; parameters that were significantly reduced by AZD4547; the immunoreactivity of ANG increased in BDL liver sections compared to WT mice. Scale bar = 5 μm. [**B**] Data are mean ± SEM of 4 *q*PCR reactions from 3 preparations of isolated cholangiocytes or total liver from 9 animals. *p<0.05 vs. the corresponding control value, #p<0.05 vs Mdr2$^{-/-}$ mice.

In vitro studies in human H69 and HSCs

In H69 cells, we looked at inflammatory markers, *IL-6*, and *IL-1β,* and *monocyte chemoattractant protein-1*, a regulatory chemokine in the migration and infiltration of macrophages. In all three genes, recombinant human FGF1 increased expression compared to untreated controls (Figure 20A). It was also noted that proliferation marker *Ki67*, angiogenesis maker, *ANG*, and fibrosis markers *Col1α1* and *TGF-β1*. Treatment with recombinant human FGF1 increased expression compared to untreated cells. For *in vitro* senescence markers we measured the gene expression of *p16*, and *p21*. Both were increased in response to 24-hour treatment with recombinant human FGF1 when compared to untreated controls (Figure 20A).

In hepatic stellate cells we also evaluated *Ki67*, *ANG*, and *MCP-1*. Like the human cholangiocytes, 24-hour exposure to recombinant human FGF1 increased expression over control cells. This pattern of expression was also seen in the markers of fibrosis *Col1α1*, *FN-1*, and *TGF-β1*, which were increased in the rhFGF1 group when compared to untreated controls (Figure 20B).

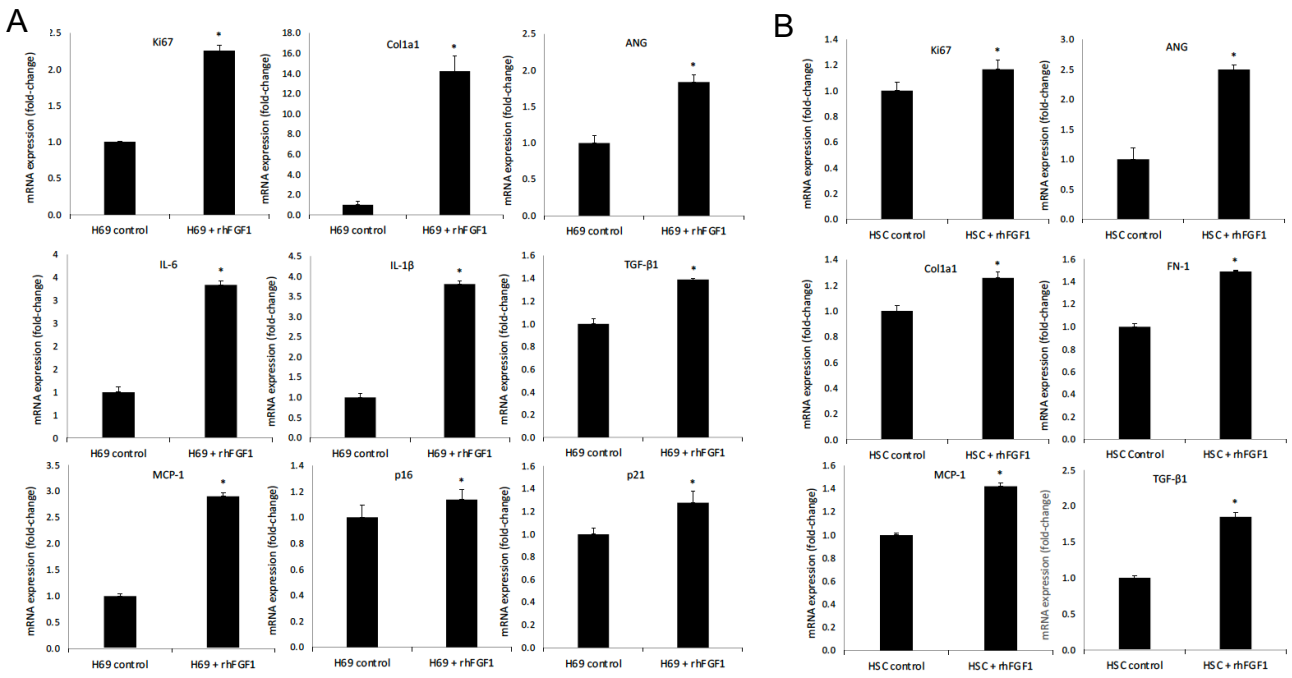

Figure 20: rhFGF1 increases proliferation, fibrosis, angiogenesis, inflammation, and senescence markers in human cell lines compared to untreated controls

[A] In H69 cells treated with rhFGF1, there was enhanced mRNA expression of proliferation, fibrosis, senescence, and angiogenesis markers compared to untreated cells. [**B**] In HSCs treated with rhFGF1, there was increased mRNA expression of proliferation, fibrosis, inflammation, and angiogenesis markers compared to untreated cells. [**A-B**] Data are mean ± SEM of 4 *q*PCR reactions from 3 preparations of H69 or HSCs. *p<.05 versus control H69 or HSCs.

FGFR1-4 and FGF1 immunoreactivity are increased in PSC patients

In Figure 21, in PSC human total liver sections, we saw increased immunoreactivity of FGF receptors 1, 2, 3, and 4 (in green), with cholangiocyte colocalization of receptors 1-3 (in red). There was also increased FGF1 immunoreactivity in the PSC samples when compared to healthy controls. This immunoreactivity was colocalized with the cholangiocytes and found in the surrounding tissue (Figure 22).

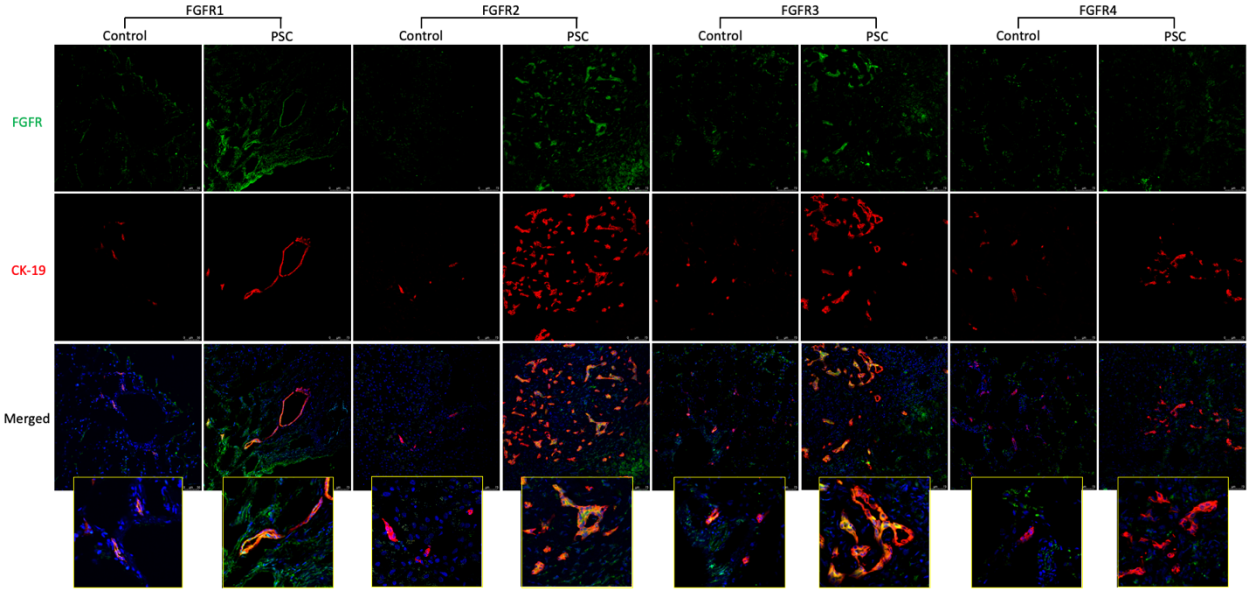

Figure 21: By immunofluorescence, PSC patients have increased immunoreactivity of FGFR 1-4 in bile ducts compared to healthy controls

There was increased FGFR1-4 immunoreactivity (co-localized with CK-19) in PSC patients compared to healthy controls. Scale bar = 75 μm.

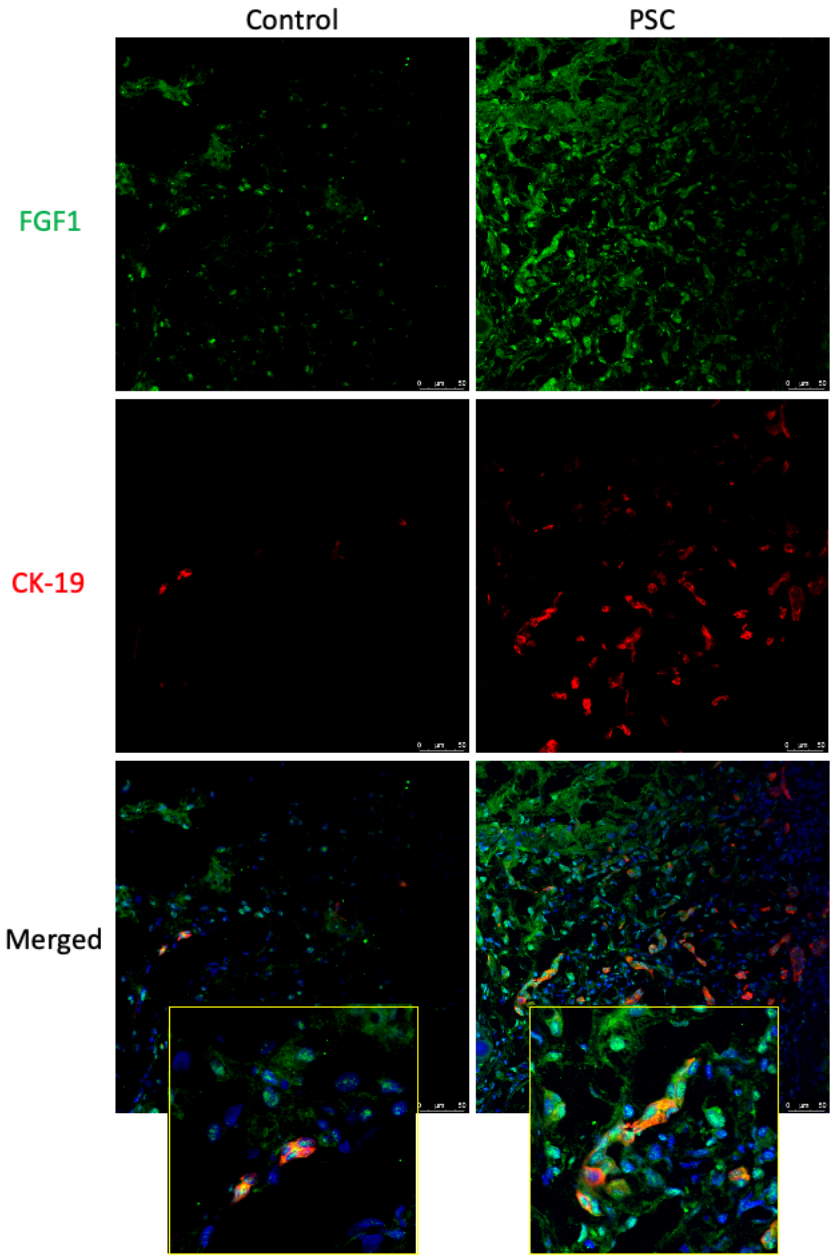

Figure 22: PSC patients have increased FGF1 immunoreactivity in bile ducts compared to healthy controls

We observed increased immunoreactivity for FGF1 in bile ducts (co-stained with CK-19) in liver sections from PSC patients compared to healthy controls. Scale bar = 75μm.

Ingenuity pathway analysis software

To explore whether there was correlation between FGF1 and miR-16 we used Ingenuity Pathway Analysis, or IPA, software by Qiagen. IPA software utilizes expansive databases created by high-throughput sequencing and microarray data. The software then surveils for pathways which can consist of activation, interaction, inhibition, and regulation between proteins, genes, drug mechanisms, or chemical compounds. The targets we entered for analysis were miR-16 and FGF1. The IPA map displayed miR-16 activation or causation interactions with FGFR1, VEGFA, and VEGFC. FGFR1 also had similar interactions with FGF1, which in turn was shown to act on or inhibit FGFR1. Details from our map showed FGF1 was shown to have indirect interaction with VEGFA, VEGF, and VEGFC (Figure 23).

There is decreased *miR-16* gene expression in isolated cholangiocytes from Mdr2$^{-/-}$ animals compared to FVB controls. BDL animals also had reduced *miR-16* expression compared to WT which was further reduced in both WT and BDL by administration with recombinant human FGF1 (Figure 24).

Similar to our animal models, there is reduced *miR-16* expression levels from total liver samples from four PSC patients when compared to four healthy controls (Figure 25).

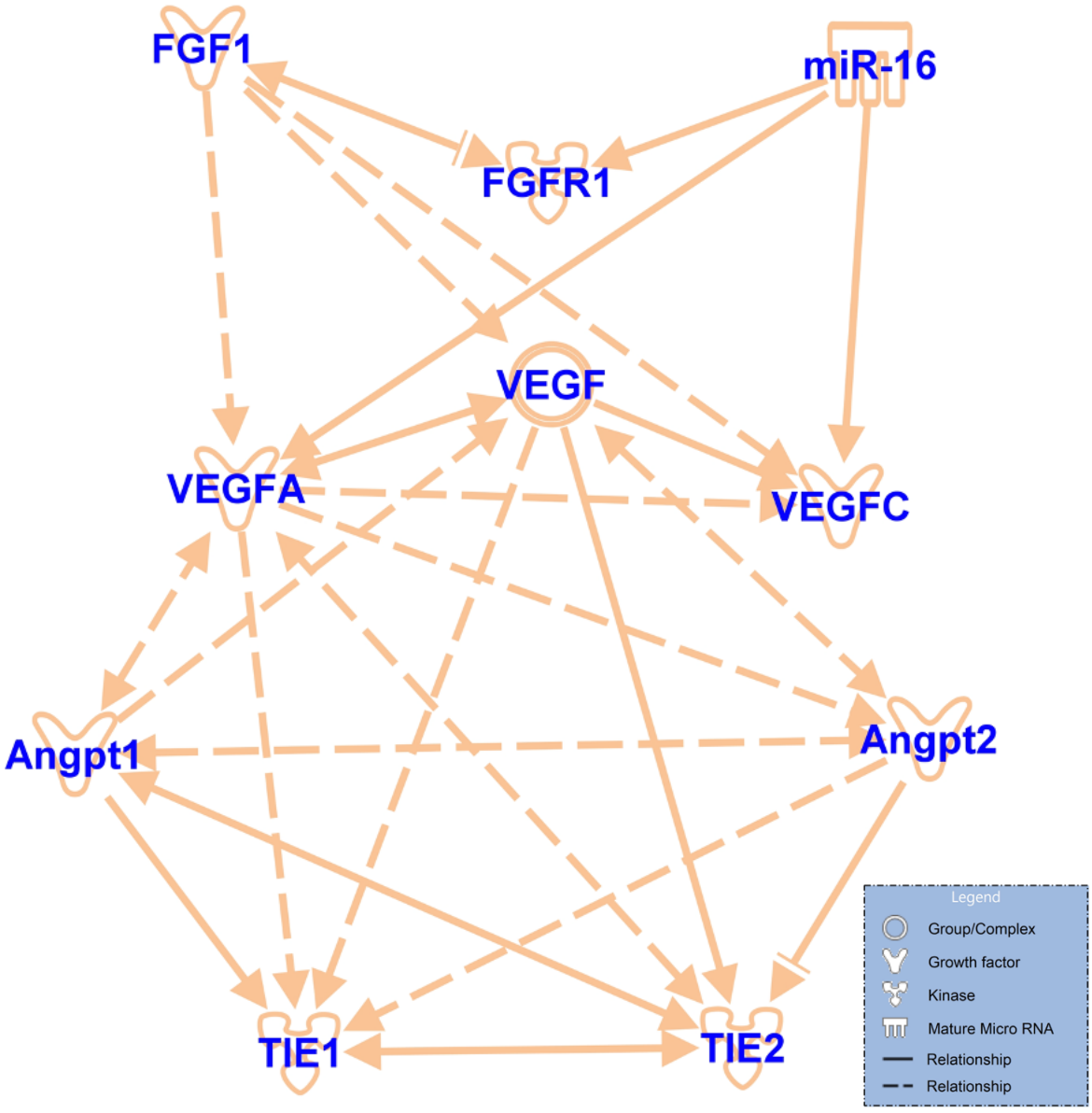

Figure 23: Ingenuity pathway analysis map

Ingenuity pathway analysis map demonstrating relational connections between FGFR1, FGF1, miR-16, and angiogenic factors.

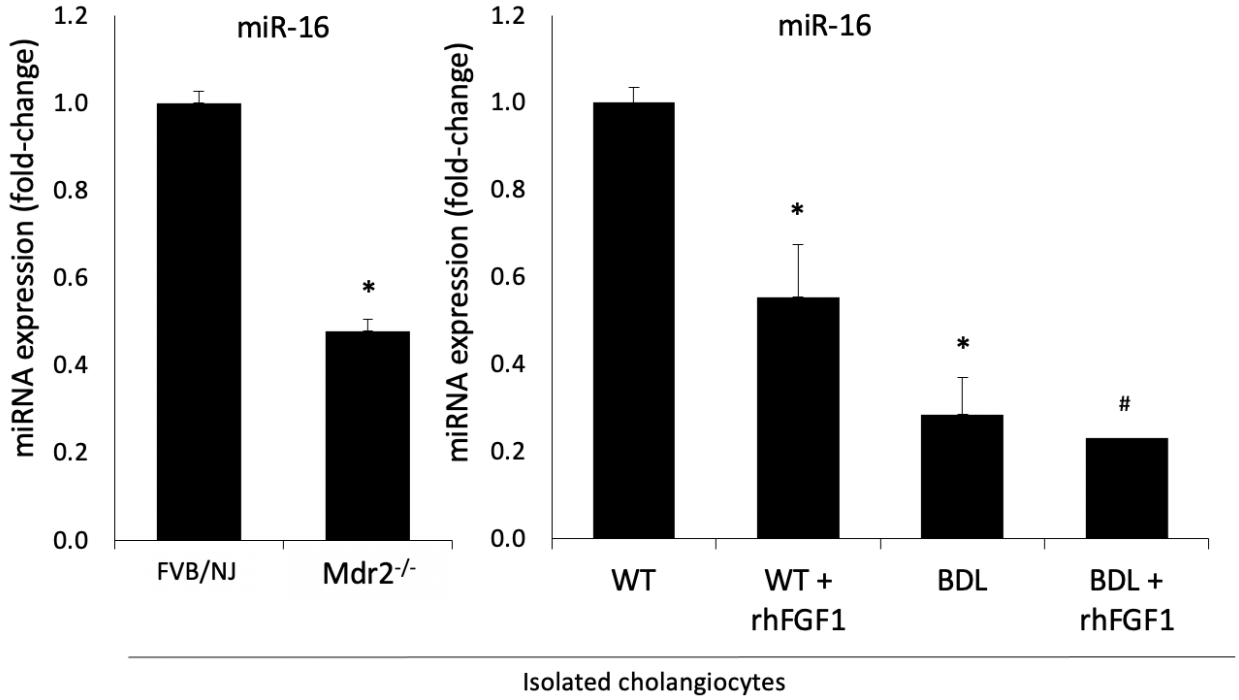

Figure 24: Chronic and acute injury decreases miR-16 expression in isolated cholangiocytes, rhFGF1 further lowers expression

There was: (i) decreased expression of *miR-16* in cholangiocytes from both BDL and Mdr2$^{-/-}$ mice compared to control mice; and (ii) reduced expression of *miR-16* in cholangiocytes from both C57BL/6 and BDL mice treated with rhFGF1 compared to the corresponding control mice. Data are mean ± SEM of 4 *q*PCR reactions from 3 cumulative preparations of isolated cholangiocytes from 9 animals. *$p<0.05$ vs. WT mice; #$p<0.05$ vs. BDL mice.

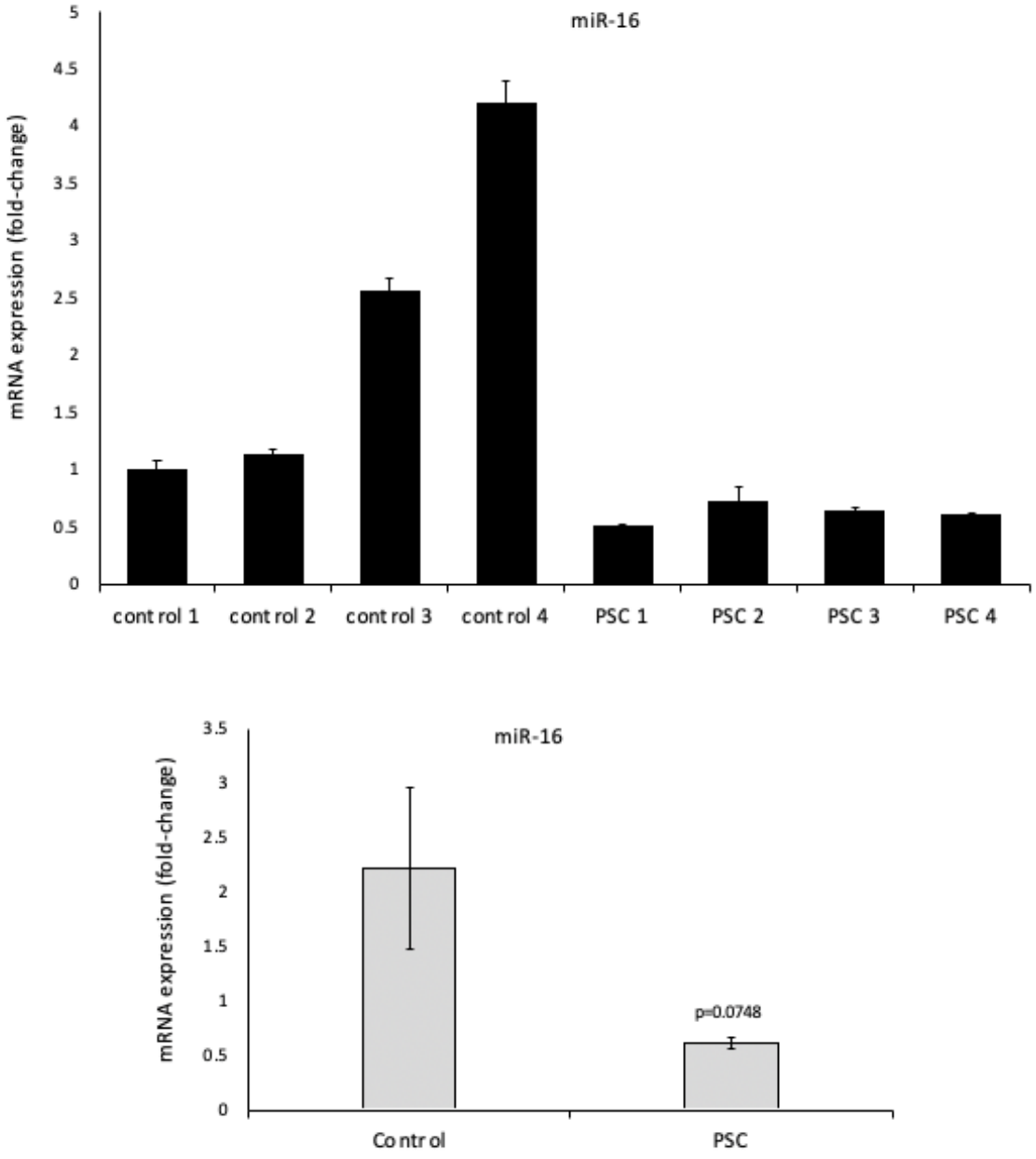

Figure 25: PSC patients have decreased miR-16 gene expression via qPCR in total liver

There was decreased expression of miR-16 in total liver samples from PSC patients compared to controls. Data are mean ± SEM of 3 experiments from serum from 4 human controls and 4 PSC patients. *p<0.05 vs. controls.

CHAPTER IV

CONCLUSIONS

To further understand the molecular underpinnings of cholangiocyte pathophysiology during cholestasis, we investigated the FGF1 pathway in cholestatic animal models and its correlation with miR-16 levels. Our study demonstrated: (i) there was an upregulation of FGFR1-4 in cholangiocytes from BDL and Mdr2$^{-/-}$ mice, with a corresponding decrease in miR-16; (ii) cholangiocytes but not HSCs displayed immunoreactivity for FGF1; (iii) administration of rhFGF1 increased ductular reaction, hepatic inflammation, and fibrosis in WT and BDL mice compared to control animals, phenotypes that were decreased following AZD4547 treatment; and (iv) increases in FGF1 serum protein, immunoreactivity in total liver, and gene expression in isolated cholangiocytes. Additionally, there were increased levels of FGF1 in supernatants collected from isolated cholangiocytes as well as increased biliary senescence/ductular reaction, hepatic inflammation, and fibrosis in Mdr2$^{-/-}$ mice; parameters that were either significantly decreased or trended down (TGF-β1 serum and gene expression levels) in response to treatment with AZD4547 or anti-FGF1 monoclonal antibody. In late-stage human PSC samples, there was increased immunoreactivity of FGFR1-4 and FGF1 and decreased expression of miR-16. *In vitro*, we have demonstrated that rhFGF1 increased the mRNA expression of proliferation, senescence, fibrosis, and angiogenesis markers in H69 cells and HSCs compared to nontreated cells. These findings attest to a critical role for FGF1 signaling in promoting biliary liver injury possibly through interaction with miR-16.

In support of our findings, several studies have demonstrated a role for various FGFs and their corresponding receptors in signaling pathways that modulate a variety of cholestatic liver diseases. [105,106,107] One such study showed the relationship between FGF15/19 and its receptor, FGFR4. Their study, like our own, demonstrated cholangiocytes express FGFR4 which in turn is activated in an autocrine fashion resulting in the regulation of sterol 27-hydroxlyase (*Cyp27)*, a regulatory bile acid biosynthesis enzyme produced by cholangiocytes. [106] In addition, FGFR1, 2, and 4 were shown to be upregulated in various CCA cell lines and to regulate CCA growth by an autocrine mechanism. [107] Parallel to our results in BDL and $Mdr2^{-/-}$ mice, several studies demonstrated a role for all four FGFRs in the activation of HSCs. [105] Our data showing increased FGF1 levels in serum and cholangiocyte supernatants are supported by numerous studies that evaluated the levels of other FGF isoforms during disease states. For instance, one such study demonstrated increased expression/serum levels of hepatic FGF19 in patients with primary biliary cholangitis (PBC) that correlated with severity of disease. [108] Similarly, FGF19 serum levels were higher in cirrhotic PBC patients compared to healthy or non-cirrhotic PBC patients. [109] Furthermore, serum FGF21 is elevated during ischemia/reperfusion-induced liver injury in patients 2 hours post-liver transplantation.[110]

The FGF family is comprised of 22 FGF members, which act as critical paracrine signals in liver pathophysiology.[111] FGF1 is a controversial and complex player. For example, one study showed that FGF1 ameliorates liver steatosis, fibrosis, and apoptosis in a diabetic mouse model of liver injury.[112] Also, FGF1 improves intrahepatic cholestasis by downregulation of bile acid levels.[113] The beneficial effects of FGF1 and other FGF

isoforms (e.g., FGF21) on steatosis and steatohepatitis were also observed in mouse models of nonalcoholic fatty liver diseases.[114] Yet another study showed that elevated levels of FGF19 suppress bile acid synthesis through inhibition of the CYP7A1 gene, thus providing beneficial effects for PBC patients. [109] Conversely, another study demonstrated overexpression of FGF19 in skeletal muscle resulted in the development of hepatocellular carcinoma in transgenic mice. [115] An additional study by Yu *et al*. revealed that animals lacking either FGF1 and/or FGF2 had significantly reduced liver fibrosis compared to control animals in a carbon tetrachloride (CCl_4)-induced chronic injury model.[116] Parallel to our findings of decreased liver fibrosis and angiogenesis with an FGFR antagonist, a recent study showed that Brivanib (a selective inhibitor of VEGF receptor and FGFR tyrosine kinases) inhibits liver fibrosis and angiogenesis through the inhibition of VEGF- and FGF-induced HSC proliferation in three unique models of liver fibrosis, including BDL. [117] Concerning the biliary epithelium, several studies demonstrated that stimulation of FGF/FGFR signaling not only has a role in the expansion of some forms of CCA but also contributes to the onset of pathological hallmarks, such as inflammation, cellular senescence, and fibrosis, during cholestatic, non-neoplastic injury.[118]

In our study, FGF1-induced liver fibrosis (observed in normal and cholestatic animals) may be due to enhanced biliary proliferation/ductular reaction and biliary senescence (concomitant with enhanced expression/levels of the SASP factor, TGF-β1), thus activating HSCs and liver fibrosis by a paracrine mechanism.[104] HSCs can be activated by a variety of cells, each providing a route for FGFR signaling. Neighboring hepatocytes can release reactive oxygen species (ROS) or TGF-β following insult or injury, driving fibrogenesis [119] which in turn overexpress FGF9 which activates FGR4 on

hepatocytes in a paracrine mechanism, which respond with an increase in TGF-β signaling. [120] An influx of Kuffer cells also contributes to HSC activation through the generation of ROS and cytokines such as TGF-β. [119] Cholangiocytes, in response to injury participate in senescence, increasing their expression of pro-inflammatory cytokines IL-6 and IL-8, [121] resulting in the increase in inflammatory cells such as Kuffer cells. [122]

On the other hand, the decrease in liver fibrosis observed in cholestatic mice after treatment with an FGFR antagonist or an anti-FGF antibody is likely due to the concomitant reduction in the ductular reaction/biliary senescence and reduced release of SASP factors. Our current and previous studies support this tight correlation between changes in ductular reaction/biliary senescence and activation of HSCs by a paracrine pathway.[94] Supporting this concept, decreased biliary senescence signaling by downregulation of p16 (an inhibitor of cyclin-dependent kinases, CDK) in $Mdr2^{-/-}$ mice by administration of p16 Vivo-Morpholino reduced ductular reaction and liver inflammation and fibrosis. [118] Research has also shown disruption of the TGF-β pathway by LY2157299, a small molecule that targets TGF-β receptors, reduces liver injury and overall senescent cell populations through macrophage clearance of senescent cells. [123]

Although we have shown that FGF1 increases liver inflammation in our cholestatic mouse models, there are contrasting data regarding the role of FGF1 signaling and inflammation. Liang *et al.* previously demonstrated reduced FGF1 serum levels in type 1 and type 2 diabetic patients, and a reduction in FGF1 protein expression and serum levels in their mouse model of renal inflammation. Furthermore, they reported treatment with FGF1 reduced diabetes-induced inflammation in the renal system. [124] Additional research has shown FGF1 can inhibit macrophage recruitment in adipose tissue decreasing the

overall inflammatory response. This was done through transcriptional down-regulation of CCL2 in adipose tissue. [125] In support of our findings, a study has shown that disruption of FGF signaling by FGFR inhibitors reduces inflammatory responses (induced by concanavalin A) in HSCs. [126]

Having demonstrated the correlation of increased FGF1 and decreased miR-16 in cholangiocytes from both BDL and Mdr2$^{-/-}$ mice, we next evaluated the expression of miR-16 with Ingenuity Pathway Analysis (IPA) software (Figure 12). IPA software utilizes expansive databases created by high-throughput sequencing and microarray data. The software then surveils for pathways representing activation, interaction, inhibition, and regulation between proteins, genes, drug mechanisms, or chemical compounds. [127] The targets we entered for analysis were miR-16 and FGF1. Our IPA map supported our reported data and displayed miR-16 activation or causation interactions through unidirectional solid arrows directed at FGFR1, VEGFA, and VEGFC. FGFR1 was also reported to have similar interactions with FGF1, which in turn was shown to act on or inhibit FGFR1 as indicated by a bi-directional arrow (Figure 23). FGF1 was shown to have indirect interaction (dashed arrows) with VEGFA, VEGF, and VEGFC. IPA predicts or reports interactional relationships so to further explore the connection between miR-16 and FGF1 we used additional commercially available TargetScan software to predict base-pairing between miR-16 and human FGF1. TargetScan reported a Context ++ score percentile of 90 out of 100. The higher the percentile score the more favorable the reported site match than any other sites on that miRNA. [128]

Like the conundrum of FGF1 in hepatic injury, there are controversial data regarding the role of miR-16 in liver injury and repair. In contrast to previous studies and

our findings showing the downregulation of miR-16 in Mdr2$^{-/-}$ and BDL mice (in cholangiocytes) and human PSC total liver samples, other studies have shown that: (i) mice with acute liver failure displayed higher levels of miR-16; and (ii) miR-16 knockdown reduced hepatic apoptosis and tumor necrosis factor synthesis by a Bcl-2-dependent mechanism.[129] The difference in miR-16 expression between this study and others (including our current findings)[99,130,131] may be due to the acute injury, and the significantly reduced time period between injury and sacrifice, hours vs. days, which likely resulted in the activation of different signaling pathways.[129] Zhu *et al.* also showed patients with active hepatis C viral infections had significant increases in miR-16 in peripheral blood mononuclear cells and commercially available cultured human liver cell lines. Using a similar network analysis program, they determined that hepatocyte growth factor and Smad7 were the targets of miR-16. They also were able to manipulate hepatocyte growth factor and Smad7 expression levels in cultured cells through mimics or inhibitors of miR-16. However, while they analyzed a cultured liver cell line, they did not determine miR-16 levels in either animal models or patient samples other than peripheral blood mononuclear cells. [132] Similar to our findings, Kim *et al*. demonstrated downregulation of miR-16 in both CCl_4-treated animals and patients with severe liver fibrosis compared to WT controls and patients with mild fibrotic phenotypes.[133] Furthermore, Hepatitis B virus X protein reduces the expression of miR-16, triggering the malignant transformation of the hepatocyte cell line HepG2 *in vitro*.[130] Lastly, recent research in a CCl_4 rat injury model has shown miR-16 regulates key signaling pathways, such as TGF-β, in the transformation of HSCs to myofibroblasts. Restoration of miR-16 in isolated

myofibroblasts decreased fibrosis-related cytokines like TGFβ2 and collagens, including Col1a1. [134]

While this project established only a correlation between miR-16 and FGF1, we did demonstrate an increase in the immunoreactivity of FGFR1-4 in cholangiocytes and HSCs in addition to upregulated cholangiocyte gene expression in our mouse models. Previous research has established lung cancer fibroblast connections between hepatocyte growth factor (HGF), miR-16, and FGFR1. Following the establishment of an HGF/miR-16 connection, researchers explored the mechanism of inhibition. They reported miR-16 transfection of CAF154-hTERT fibroblasts significantly reduced the FGFR1 protein expression via western blot while leaving FGF1 and -2 ligand expression intact. Their data also showed the connection between HGF and miR-16 was the miR-16 regulation of MEK1 which then regulated HGF secretion. They concluded miR-16 possibly regulated HGF through the regulation of downstream targets FGFR1 and MEK1. [135] Chamorro-Jorganes *et al* also reported miR-16 overexpression in human umbilical vein endothelial cells significantly decreased the mRNA expression of *FGFR1*. They further demonstrated inhibition of miR-16 resulted in significant increases of FGFR1 via western blot and *q*PCR. Furthermore, they suggested miR-16 controls proliferation and migration of endothelial cells through FGFR1 signaling. [136] Lastly, mesothelioma, an aggressive malignancy with limited treatment options has been previously shown to have downregulation of miR-15/16 family. TargetScan reported FGFR1 and 4 to be predicted targets of miR-16 so using mimics in mesothelioma cells *in vitro*, researchers confirmed a corresponding decrease in FGFR1 and 4. They then went on to target a combination of

FGFR1 and the well-established miR-16 target, Bcl-2, *in vitro* and found a synergistic effect on the cancer cell growth. [137]

In summary, we have shown that treatment with rhFGF1 increases PSC phenotypes in a mechanical injury mouse model, while treatment with the FGFR antagonist AZD4547 decreased these phenotypes in both BDL and Mdr2$^{-/-}$ animals. Furthermore, we demonstrated an inverse correlation in FGF1 and miR-16 levels from isolated cholangiocytes. Due to the duplicitous roles both FGF1 and miR-16 play in various inflammatory/fibrotic conditions there is ample opportunity for future research endeavors in this area. One potential target that may prove useful in identifying the link between miR-16 and FGF1 is the role of HSCs. Further exploration might include determining molecular crosstalk between cholangiocytes and HSCs and the role of miR-16 utilizing extracellular vesicle isolation and analysis. Manipulation of miR-16 *in vitro* and *in vivo*, with either transfected inhibitors, mimics, or vivo morpholinos, along with more broad analysis such as gene arrays, protein profiler assays, and luciferase assays may aid in targeting individual pathways or determining protein/genetic response. With this information, modulation of miR-16 through an FGF1-mediated pathway may yield new therapeutic targets for managing cholangiopathies such as PSC.

REFERENCES

1 Lazaridis, K. N. & LaRusso, N. F. The Cholangiopathies. *Mayo Clinic Proceedings* **90**, 791-800, doi:10.1016/j.mayocp.2015.03.017 (2015).

2 O'Hara, S. P., Tabibian, J. H., Splinter, P. L. & LaRusso, N. F. The dynamic biliary epithelia: Molecules, pathways, and disease. *Journal of Hepatology* **58**, 575-582, doi:https://doi.org/10.1016/j.jhep.2012.10.011 (2013).

3 Yokoda, R. T., Carey, Elizabeth J. Primary Biliary Cholangitis and Primary Sclerosing Cholangitis. *The American Journal of Gastroenterology* **114**, 1593-1605, doi:10.14309/ajg.0000000000000268 (2019).

4 Hirschfield, G. M., Karlsen, T. H., Lindor, K. D. & Adams, D. H. Primary sclerosing cholangitis. *The Lancet* **382**, 1587-1599, doi:https://doi.org/10.1016/S0140-6736(13)60096-3 (2013).

5 Karlsen, T. H., Folseraas, T., Thorburn, D. & Vesterhus, M. Primary sclerosing cholangitis – a comprehensive review. *Journal of Hepatology* **67**, 1298-1323, doi:https://doi.org/10.1016/j.jhep.2017.07.022 (2017).

6 Eaton, J. E., Talwalkar, J. A., Lazaridis, K. N., Gores, G. J. & Lindor, K. D. Pathogenesis of primary sclerosing cholangitis and advances in diagnosis and management. *Gastroenterology* **145**, 521-536, doi:10.1053/j.gastro.2013.06.052 (2013).

7 Zein, C. O. & Lindor, K. D. Latest and Emerging Therapies for Primary Biliary Cirrhosis and Primary Sclerosing Cholangitis. *Current Gastroenterology Reports* **12**, 13-22, doi:10.1007/s11894-009-0079-2 (2010).

8 Romil Saxena, N. T. Canals of Hering: Recent Insights and Current Knowledge. *Seminars in LIver Disease* **24**, 43-48, doi:10.1055/s-2004-823100 (2004).

9 Tabibian, J. H., Masyuk, A. I., Masyuk, T. V., O'Hara, S. P. & LaRusso, N. F. Physiology of cholangiocytes. *Compr Physiol* **3**, 541-565, doi:10.1002/cphy.c120019 (2013).

10 Maroni, L. *et al.* Functional and structural features of cholangiocytes in health and disease. *Cell Mol Gastroenterol Hepatol* **1**, 368-380, doi:10.1016/j.jcmgh.2015.05.005 (2015).

11 Tabibian, J. H., Masyuk, A. I., Masyuk, T. V., O'Hara, S. P. & LaRusso, N. F. Physiology of cholangiocytes. *Compr Physiol* **3**, 541-565, doi:10.1002/cphy.c120019 (2013).

12 Alpini, G. *et al.* Morphological, molecular, and functional heterogeneity of cholangiocytes from normal rat liver. *Gastroenterology* **110**, 1636-1643, doi:https://doi.org/10.1053/gast.1996.v110.pm8613073 (1996).

13 Sato, K., Meng, F., Giang, T., Glaser, S. & Alpini, G. Mechanisms of cholangiocyte responses to injury. *Biochimica et Biophysica Acta (BBA) -*

Molecular Basis of Disease **1864**, 1262-1269, doi:https://doi.org/10.1016/j.bbadis.2017.06.017 (2018).

14 Yoo, K. S., Lim, W. T. & Choi, H. S. Biology of Cholangiocytes: From Bench to Bedside. *Gut Liver* **10**, 687-698, doi:10.5009/gnl16033 (2016).

15 Mancinelli, R. *et al.* After Damage of Large Bile Ducts by Gamma-Aminobutyric Acid, Small Ducts Replenish the Biliary Tree by Amplification of Calcium-Dependent Signaling and de Novo Acquisition of Large Cholangiocyte Phenotypes. *The American Journal of Pathology* **176**, 1790-1800, doi:https://doi.org/10.2353/ajpath.2010.090677 (2010).

16 Alpini, G. *et al.* Heterogeneity of the proliferative capacity of rat cholangiocytes after bile duct ligation. *American Journal of Physiology-Gastrointestinal and Liver Physiology* **274**, G767-G775, doi:10.1152/ajpgi.1998.274.4.G767 (1998).

17 Masyuk, A. I., Masyuk, T. V. & LaRusso, N. F. Cholangiocyte primary cilia in liver health and disease. *Dev Dyn* **237**, 2007-2012, doi:10.1002/dvdy.21530 (2008).

18 Roger Chapman, J. F., Anthony Kalloo, David M. Nagorney, Kirsten Muri Boberg, Benjamin Shneider, and Gregory J. Gores. Diagnosis and Management of Primary Sclerosing Cholangitis. *Hepatology* **51**, 660-678, doi:10.1002/hep.23294 (2010).

19 Boberg, K. M. *et al.* Features of autoimmune hepatitis in primary sclerosing cholangitis: An evaluation of 114 primary sclerosing cholangitis

patients according to a scoring system for the diagnosis of autoimmune hepatitis. *Hepatology* **23**, 1369-1376, doi:https://doi.org/10.1002/hep.510230612 (1996).

20 Roskams, T. & Desmet, V. Ductular reaction and its diagnostic significance. *Semin Diagn Pathol* **15**, 259-269 (1998).

21 Govaere, O. *et al.* High-throughput sequencing identifies aetiology-dependent differences in ductular reaction in human chronic liver disease. *The Journal of pathology* **248**, 66-76, doi:10.1002/path.5228 (2019).

22 Jiao, J., Friedman, S. L. & Aloman, C. Hepatic fibrosis. *Curr Opin Gastroenterol* **25**, 223-229, doi:10.1097/mog.0b013e3283279668 (2009).

23 Ezhilarasan, D., Sokal, E. & Najimi, M. Hepatic fibrosis: It is time to go with hepatic stellate cell-specific therapeutic targets. *Hepatobiliary & Pancreatic Diseases International* **17**, 192-197, doi:https://doi.org/10.1016/j.hbpd.2018.04.003 (2018).

24 Brenner, D. A. *et al.* New aspects of hepatic fibrosis. *Journal of Hepatology* **32**, 32-38, doi:https://doi.org/10.1016/S0168-8278(00)80413-4 (2000).

25 Li, H. Angiogenesis in the progression from liver fibrosis to cirrhosis and hepatocelluar carcinoma. *Expert Review of Gastroenterology & Hepatology* **15**, 217-233, doi:10.1080/17474124.2021.1842732 (2021).

26 Elpek, G. Ö. Angiogenesis and liver fibrosis. *World J Hepatol* **7**, 377-391, doi:10.4254/wjh.v7.i3.377 (2015).

27 Medina, J., Arroyo, A. G., Sánchez-Madrid, F. & Moreno-Otero, R. Angiogenesis in chronic inflammatory liver disease. *Hepatology* **39**, 1185-1195, doi:https://doi.org/10.1002/hep.20193 (2004).

28 Ribatti, D. & Crivellato, E. Immune cells and angiogenesis. *J Cell Mol Med* **13**, 2822-2833, doi:10.1111/j.1582-4934.2009.00810.x (2009).

29 Mejias, M. *et al.* Beneficial effects of sorafenib on splanchnic, intrahepatic, and portocollateral circulations in portal hypertensive and cirrhotic rats. *Hepatology* **49**, 1245-1256, doi:10.1002/hep.22758 (2009).

30 Dyson, J. K., Beuers, U., Jones, D. E. J., Lohse, A. W. & Hudson, M. Primary sclerosing cholangitis. *The Lancet* **391**, 2547-2559, doi:https://doi.org/10.1016/S0140-6736(18)30300-3 (2018).

31 Koyama, Y. & Brenner, D. A. Liver inflammation and fibrosis. *J Clin Invest* **127**, 55-64, doi:10.1172/JCI88881 (2017).

32 Pinto, C., Giordano, D. M., Maroni, L. & Marzioni, M. Role of inflammation and proinflammatory cytokines in cholangiocyte pathophysiology. *Biochimica et Biophysica Acta (BBA) - Molecular Basis of Disease* **1864**, 1270-1278, doi:https://doi.org/10.1016/j.bbadis.2017.07.024 (2018).

33 Di Micco, R., Krizhanovsky, V., Baker, D. & d'Adda di Fagagna, F. Cellular senescence in ageing: from mechanisms to therapeutic opportunities. *Nature Reviews Molecular Cell Biology* **22**, 75-95, doi:10.1038/s41580-020-00314-w (2021).

34 Dulic, V. Senescence Regulation by mTOR. *Methods in molecular biology (Clifton, N.J.)* **965**, 15-35, doi:10.1007/978-1-62703-239-1_2 (2013).

35 Campisi, J. & d'Adda di Fagagna, F. Cellular senescence: when bad things happen to good cells. *Nature Reviews Molecular Cell Biology* **8**, 729-740, doi:10.1038/nrm2233 (2007).

36 Laish, I. *et al.* Increased TERC gene copy number and cells in senescence in primary sclerosing cholangitis compared to colitis and control patients. *Gene* **529**, 245-249, doi:https://doi.org/10.1016/j.gene.2013.07.098 (2013).

37 Lopes-Paciencia, S. *et al.* The senescence-associated secretory phenotype and its regulation. *Cytokine* **117**, 15-22, doi:https://doi.org/10.1016/j.cyto.2019.01.013 (2019).

38 Sato, K. *et al.* Preclinical insights into cholangiopathies: disease modeling and emerging therapeutic targets. *Expert Opin Ther Targets* **23**, 461-472, doi:10.1080/14728222.2019.1608950 (2019).

39 Tabibian, J. H. & Bowlus, C. L. Primary sclerosing cholangitis: A review and update. *Liver Res* **1**, 221-230, doi:10.1016/j.livres.2017.12.002 (2017).

40 Tag, C. G. *et al.* Bile duct ligation in mice: induction of inflammatory liver injury and fibrosis by obstructive cholestasis. *J Vis Exp*, 52438, doi:10.3791/52438 (2015).

41 Mariotti, V., Strazzabosco, M., Fabris, L. & Calvisi, D. F. Animal models of biliary injury and altered bile acid metabolism. *Biochim Biophys Acta Mol Basis Dis* **1864**, 1254-1261, doi:10.1016/j.bbadis.2017.06.027 (2018).

42 Pose, E., Sancho-Bru, P. & Coll, M. in *Experimental Cholestasis Research* (ed Mathieu Vinken) 249-257 (Springer New York, 2019).

43 Laure-Alix Clerbaux, N. V. H., Annette S.H. Gouw, Rita Manco, Regina Español-Suñer and Isabelle A. Leclercq Relevance of the CDE and DDC Mouse Models to Study Ductular Reaction in Chronic Human Liver Diseases, Experimental Animal Models of Human Diseases - An Effective Therapeutic Strategy. *IntechOpen*, doi:10.5772/intechopen.69533 (2017).

44 Fickert, P. *et al.* Lithocholic acid feeding induces segmental bile duct obstruction and destructive cholangitis in mice. *The American journal of pathology* **168**, 410-422, doi:10.2353/ajpath.2006.050404 (2006).

45 Fickert, P. *et al.* Characterization of animal models for primary sclerosing cholangitis (PSC). *Journal of hepatology* **60**, 1290-1303, doi:10.1016/j.jhep.2014.02.006 (2014).

46 Morita, S.-y. & Terada, T. Molecular mechanisms for biliary phospholipid and drug efflux mediated by ABCB4 and bile salts. *Biomed Res Int* **2014**, 954781-954781, doi:10.1155/2014/954781 (2014).

47 Popov, Y., Patsenker, E., Fickert, P., Trauner, M. & Schuppan, D. Mdr2 (Abcb4)-/- mice spontaneously develop severe biliary fibrosis via massive

dysregulation of pro- and antifibrogenic genes. *Journal of Hepatology* **43**, 1045-1054, doi:https://doi.org/10.1016/j.jhep.2005.06.025 (2005).

48 Liedtke, C. *et al.* Experimental liver fibrosis research: update on animal models, legal issues and translational aspects. *Fibrogenesis & Tissue Repair* **6**, 19, doi:10.1186/1755-1536-6-19 (2013).

49 Blanco, P. G. *et al.* Induction of colitis in cftr−/− mice results in bile duct injury. *American Journal of Physiology-Gastrointestinal and Liver Physiology* **287**, G491-G496, doi:10.1152/ajpgi.00452.2003 (2004).

50 Durie, P. R., Kent, G., Phillips, M. J. & Ackerley, C. A. Characteristic multiorgan pathology of cystic fibrosis in a long-living cystic fibrosis transmembrane regulator knockout murine model. *The American journal of pathology* **164**, 1481-1493, doi:10.1016/S0002-9440(10)63234-8 (2004).

51 Rondeau, M. P. Hepatitis and Cholangiohepatitis. *Small Animal Critical Care Medicine*, 610-614, doi:10.1016/B978-1-4557-0306-7.00115-X (2015).

52 Otte, C. M. *et al.* Immunohistochemical evaluation of the activation of hepatic progenitor cells and their niche in feline lymphocytic cholangitis. *J Feline Med Surg* **20**, 30-37, doi:10.1177/1098612x17699723 (2018).

53 Arenas-Gamboa, A. M. *et al.* Sclerosing cholangitis in baboons (Papio spp) resembling primary sclerosing cholangitis of humans. *Vet Pathol* **49**, 524-527, doi:10.1177/0300985811419532 (2012).

54 Yun, Y.-R. *et al.* Fibroblast growth factors: biology, function, and application for tissue regeneration. *J Tissue Eng* **2010**, 218142-218142, doi:10.4061/2010/218142 (2010).

55 L'Hôte, C. G. M. & Knowles, M. A. Cell responses to FGFR3 signalling: growth, differentiation and apoptosis. *Experimental Cell Research* **304**, 417-431, doi:https://doi.org/10.1016/j.yexcr.2004.11.012 (2005).

56 Sarabipour, S. & Hristova, K. Mechanism of FGF receptor dimerization and activation. *Nature Communications* **7**, 10262, doi:10.1038/ncomms10262 (2016).

57 Pellegrini, L. Role of heparan sulfate in fibroblast growth factor signalling: a structural view. *Current Opinion in Structural Biology* **11**, 629-634, doi:https://doi.org/10.1016/S0959-440X(00)00258-X (2001).

58 Powers, C. J., McLeskey, S. W. & Wellstein, A. Fibroblast growth factors, their receptors and signaling. *Endocrine-related cancer Endocr Relat Cancer Endocr. Relat. Cancer* **7**, 165-197 (2000).

59 Raju, R. *et al.* A Network Map of FGF-1/FGFR Signaling System. *J Signal Transduct* **2014**, 962962-962962, doi:10.1155/2014/962962 (2014).

60 Ornitz, D. M. & Itoh, N. The Fibroblast Growth Factor signaling pathway. *Wiley Interdiscip Rev Dev Biol* **4**, 215-266, doi:10.1002/wdev.176 (2015).

61 Gasser, E., Moutos, C. P., Downes, M. & Evans, R. M. FGF1 — a new weapon to control type 2 diabetes mellitus. *Nature Reviews Endocrinology* **13**, 599-609, doi:10.1038/nrendo.2017.78 (2017).

62 Wang, X. *et al.* FGF1 protects against APAP-induced hepatotoxicity via suppression of oxidative and endoplasmic reticulum stress. *Clinics and Research in Hepatology and Gastroenterology* **43**, 707-714, doi:https://doi.org/10.1016/j.clinre.2019.03.006 (2019).

63 He, S. *et al.* Heparinized silk fibroin hydrogels loading FGF1 promote the wound healing in rats with full-thickness skin excision. *BioMedical Engineering OnLine* **18**, 97, doi:10.1186/s12938-019-0716-4 (2019).

64 Jonker, J. W. *et al.* A PPARγ-FGF1 axis is required for adaptive adipose remodelling and metabolic homeostasis. *Nature* **485**, 391-394, doi:10.1038/nature10998 (2012).

65 Itoh, T. *et al.* Biological Effects of IL-26 on T Cell–Mediated Skin Inflammation, Including Psoriasis. *Journal of Investigative Dermatology* **139**, 878-889, doi:https://doi.org/10.1016/j.jid.2018.09.037 (2019).

66 Malemud, C. J. Growth hormone, VEGF and FGF: Involvement in rheumatoid arthritis. *Clinica Chimica Acta* **375**, 10-19, doi:https://doi.org/10.1016/j.cca.2006.06.033 (2007).

67 Bai, Y.-P. *et al.* FGF-1/-3/FGFR4 signaling in cancer-associated fibroblasts promotes tumor progression in colon cancer through Erk and MMP-7. *Cancer Science* **106**, 1278-1287, doi:https://doi.org/10.1111/cas.12745 (2015).

68 Helsten, T., Schwaederle, M. & Kurzrock, R. Fibroblast growth factor receptor signaling in hereditary and neoplastic disease: biologic and

clinical implications. *Cancer Metastasis Rev* **34**, 479-496, doi:10.1007/s10555-015-9579-8 (2015).

69 Horvitz, H. R. & Sulston, J. E. Isolation and genetic characterization of cell-lineage mutants of the nematode Caenorhabditis elegans. *Genetics* **96**, 435-454 (1980).

70 Hammond, S. M. An overview of microRNAs. *Adv Drug Deliv Rev* **87**, 3-14, doi:10.1016/j.addr.2015.05.001 (2015).

71 O'Brien, J., Hayder, H., Zayed, Y. & Peng, C. Overview of MicroRNA Biogenesis, Mechanisms of Actions, and Circulation. *Frontiers in Endocrinology* **9**, doi:10.3389/fendo.2018.00402 (2018).

72 Kim, Y. & Kim, V. N. MicroRNA Factory: RISC Assembly from Precursor MicroRNAs. *Molecular Cell* **46**, 384-386, doi:https://doi.org/10.1016/j.molcel.2012.05.012 (2012).

73 Correia de Sousa, M., Gjorgjieva, M., Dolicka, D., Sobolewski, C. & Foti, M. Deciphering miRNAs' Action through miRNA Editing. *International journal of molecular sciences* **20**, 6249, doi:10.3390/ijms20246249 (2019).

74 M, J. R. Functions and epigenetic aspects of miR-15/16: Possible future cancer therapeutics. *Gene Reports* **12**, 149-164, doi:https://doi.org/10.1016/j.genrep.2018.06.012 (2018).

75 Lages, E. *et al.* MicroRNAs: molecular features and role in cancer. *Front Biosci (Landmark Ed)* **17**, 2508-2540, doi:10.2741/4068 (2012).

76 Aqeilan, R. I., Calin, G. A. & Croce, C. M. miR-15a and miR-16-1 in cancer: discovery, function and future perspectives. *Cell Death & Differentiation* **17**, 215-220, doi:10.1038/cdd.2009.69 (2010).

77 Calin, G. A. *et al.* Frequent deletions and down-regulation of micro- RNA genes miR15 and miR16 at 13q14 in chronic lymphocytic leukemia. *Proc Natl Acad Sci U S A* **99**, 15524-15529, doi:10.1073/pnas.242606799 (2002).

78 Yan, L. *et al.* The role of microRNA-16 in the pathogenesis of autoimmune diseases: A comprehensive review. *Biomedicine & Pharmacotherapy* **112**, 108583, doi:https://doi.org/10.1016/j.biopha.2019.01.044 (2019).

79 Liang, X. *et al.* MicroRNA-16 suppresses the activation of inflammatory macrophages in atherosclerosis by targeting PDCD4. *Int J Mol Med* **37**, 967-975, doi:10.3892/ijmm.2016.2497 (2016).

80 Schönauen, K. *et al.* Circulating and Fecal microRNAs as Biomarkers for Inflammatory Bowel Diseases. *Inflammatory Bowel Diseases* **24**, 1547-1557, doi:10.1093/ibd/izy046 (2018).

81 Tsuchida, T. & Friedman, S. L. Mechanisms of hepatic stellate cell activation. *Nature Reviews Gastroenterology & Hepatology* **14**, 397-411, doi:10.1038/nrgastro.2017.38 (2017).

82 Pan, Q. *et al.* miR-16 integrates signal pathways in myofibroblasts: determinant of cell fate necessary for fibrosis resolution. *Cell Death Dis* **11**, 639-639, doi:10.1038/s41419-020-02832-z (2020).

83 Crosby, H. A. *et al.* Immunolocalization of putative human liver progenitor cells in livers from patients with end-stage primary biliary cirrhosis and sclerosing cholangitis using the monoclonal antibody OV-6. *The American journal of pathology* **152**, 771-779 (1998).

84 B. Cheng, F. D., C.-Y. Huang, H. Xiao, F.-Y. Fei, J. Li. Role of miR-16-5p in the proliferation and metastasis of hepatocellular carcinoma. *Eur Rev Med Pharmacol Sci* **23**, 137-145, doi:10.26355/eurrev_201901_16757 (2019).

85 Nelson, A. L., Dhimolea, E. & Reichert, J. M. Development trends for human monoclonal antibody therapeutics. *Nat Rev Drug Discov* **9**, 767-774, doi:10.1038/nrd3229 (2010).

86 Gavine, P. R. *et al.* AZD4547: an orally bioavailable, potent, and selective inhibitor of the fibroblast growth factor receptor tyrosine kinase family. *Cancer Res* **72**, 2045-2056, doi:10.1158/0008-5472.Can-11-3034 (2012).

87 Alpini, G., Lenzi, R., Sarkozi, L. & Tavoloni, N. Biliary physiology in rats with bile ductular cell hyperplasia. Evidence for a secretory function of proliferated bile ductules. *J Clin Invest* **81**, 569-578, doi:10.1172/jci113355 (1988).

88 Fan, L. *et al.* Fibroblast Growth Factor-1 Improves Insulin Resistance via Repression of JNK-Mediated Inflammation. *Frontiers in pharmacology* **10**, 1478-1478, doi:10.3389/fphar.2019.01478 (2019).

89 Huang, C. *et al.* A novel fibroblast growth factor-1 ligand with reduced heparin binding protects the heart against ischemia-reperfusion injury in the presence of heparin co-administration. *Cardiovasc Res* **113**, 1585-1602, doi:10.1093/cvr/cvx165 (2017).

90 Dunstan, C. R. *et al.* Systemic Administration of Acidic Fibroblast Growth Factor (FGF-1) Prevents Bone Loss and Increases New Bone Formation in Ovariectomized Rats. *Journal of Bone and Mineral Research* **14**, 953-959, doi:https://doi.org/10.1359/jbmr.1999.14.6.953 (1999).

91 Yao, T. J. *et al.* AZD-4547 exerts potent cytostatic and cytotoxic activities against fibroblast growth factor receptor (FGFR)-expressing colorectal cancer cells. *Tumour Biol* **36**, 5641-5648, doi:10.1007/s13277-015-3237-1 (2015).

92 Schoch, A., Thorey, I. S., Engert, J., Winter, G. & Emrich, T. Comparison of the lateral tail vein and the retro-orbital venous sinus routes of antibody administration in pharmacokinetic studies. *Lab Anim (NY)* **43**, 95-99, doi:10.1038/laban.481 (2014).

93 Zhou, T. *et al.* Knockdown of vimentin reduces mesenchymal phenotype of cholangiocytes in the Mdr2(-/-) mouse model of primary sclerosing

cholangitis (PSC). *EBioMedicine* **48**, 130-142, doi:10.1016/j.ebiom.2019.09.013 (2019).

94 Wu, N. *et al.* Functional Role of the Secretin/Secretin Receptor Signaling During Cholestatic Liver Injury. *Hepatology* **72**, 2219-2227, doi:10.1002/hep.31484 (2020).

95 Kennedy, L. *et al.* Amelioration of Large Bile Duct Damage by Histamine-2 Receptor Vivo-Morpholino Treatment. *Am J Pathol* **190**, 1018-1029, doi:10.1016/j.ajpath.2020.01.013 (2020).

96 Glaser, S. *et al.* Knockout of secretin receptor reduces large cholangiocyte hyperplasia in mice with extrahepatic cholestasis induced by bile duct ligation. *Hepatology* **52**, 204-214, doi:10.1002/hep.23657 (2010).

97 Nallagangula, K. S., Nagaraj, S. K., Venkataswamy, L. & Chandrappa, M. Liver fibrosis: a compilation on the biomarkers status and their significance during disease progression. *Future Sci OA* **4**, Fso250, doi:10.4155/fsoa-2017-0083 (2018).

98 Schelch, K. *et al.* A link between the fibroblast growth factor axis and the miR-16 family reveals potential new treatment combinations in mesothelioma. *Mol Oncol* **12**, 58-73, doi:10.1002/1878-0261.12150 (2018).

99 Guo, C. J., Pan, Q., Li, D. G., Sun, H. & Liu, B. W. miR-15b and miR-16 are implicated in activation of the rat hepatic stellate cell: An essential role

for apoptosis. *J Hepatol* **50**, 766-778, doi:10.1016/j.jhep.2008.11.025 (2009).

100 Kinoshita, M. *et al.* Characterization of two F4/80-positive Kupffer cell subsets by their function and phenotype in mice. *J Hepatol* **53**, 903-910, doi:10.1016/j.jhep.2010.04.037 (2010).

101 Koyama, Y. & Brenner, D. A. Liver inflammation and fibrosis. *J Clin Invest* **127**, 55-64, doi:10.1172/jci88881 (2017).

102 Huda, N. *et al.* Hepatic senescence, the good and the bad. *World J Gastroenterol* **25**, 5069-5081, doi:10.3748/wjg.v25.i34.5069 (2019).

103 Ehrlich, L. *et al.* α7-nAChR Knockout Mice Decreases Biliary Hyperplasia and Liver Fibrosis in Cholestatic Bile Duct-Ligated Mice. *Gene Expr* **18**, 197-207, doi:10.3727/105221618x15216453076707 (2018).

104 Wan, Y. *et al.* Substance P increases liver fibrosis by differential changes in senescence of cholangiocytes and hepatic stellate cells. *Hepatology* **66**, 528-541, doi:10.1002/hep.29138 (2017).

105 Lin, N. *et al.* NP603, a novel and potent inhibitor of FGFR1 tyrosine kinase, inhibits hepatic stellate cell proliferation and ameliorates hepatic fibrosis in rats. *Am J Physiol Cell Physiol* **301**, C469-477, doi:10.1152/ajpcell.00452.2010 (2011).

106 Jung, D. *et al.* FXR-induced secretion of FGF15/19 inhibits CYP27 expression in cholangiocytes through p38 kinase pathway. *Pflugers Arch* **466**, 1011-1019, doi:10.1007/s00424-013-1364-3 (2014).

107 Rizvi, S. *et al.* A Hippo and Fibroblast Growth Factor Receptor Autocrine Pathway in Cholangiocarcinoma. *J Biol Chem* **291**, 8031-8047, doi:10.1074/jbc.M115.698472 (2016).

108 Wunsch, E. *et al.* Expression of hepatic Fibroblast Growth Factor 19 is enhanced in Primary Biliary Cirrhosis and correlates with severity of the disease. *Sci Rep* **5**, 13462, doi:10.1038/srep13462 (2015).

109 Li, Z. *et al.* Circulating FGF19 closely correlates with bile acid synthesis and cholestasis in patients with primary biliary cirrhosis. *PLoS One* **12**, e0178580, doi:10.1371/journal.pone.0178580 (2017).

110 Ye, D. *et al.* Circulating Fibroblast Growth Factor 21 Is A Sensitive Biomarker for Severe Ischemia/reperfusion Injury in Patients with Liver Transplantation. *Sci Rep* **6**, 19776, doi:10.1038/srep19776 (2016).

111 Itoh, N., Nakayama, Y. & Konishi, M. Roles of FGFs As Paracrine or Endocrine Signals in Liver Development, Health, and Disease. *Front Cell Dev Biol* **4**, 30, doi:10.3389/fcell.2016.00030 (2016).

112 Xu, Z. *et al.* Fibroblast Growth Factor 1 Ameliorates Diabetes-Induced Liver Injury by Reducing Cellular Stress and Restoring Autophagy. *Front Pharmacol* **11**, 52, doi:10.3389/fphar.2020.00052 (2020).

113 Lin, H. *et al.* Paracrine Fibroblast Growth Factor 1 Functions as Potent Therapeutic Agent for Intrahepatic Cholestasis by Downregulating Synthesis of Bile Acid. *Front Pharmacol* **10**, 1515, doi:10.3389/fphar.2019.01515 (2019).

114 Bao, L. *et al.* A long-acting FGF21 alleviates hepatic steatosis and inflammation in a mouse model of non-alcoholic steatohepatitis partly through an FGF21-adiponectin-IL17A pathway. *Br J Pharmacol* **175**, 3379-3393, doi:10.1111/bph.14383 (2018).

115 Nicholes, K. *et al.* A mouse model of hepatocellular carcinoma: ectopic expression of fibroblast growth factor 19 in skeletal muscle of transgenic mice. *Am J Pathol* **160**, 2295-2307, doi:10.1016/s0002-9440(10)61177-7 (2002).

116 Yu, C. *et al.* Role of fibroblast growth factor type 1 and 2 in carbon tetrachloride-induced hepatic injury and fibrogenesis. *Am J Pathol* **163**, 1653-1662, doi:10.1016/s0002-9440(10)63522-5 (2003).

117 Nakamura, I. *et al.* Brivanib attenuates hepatic fibrosis in vivo and stellate cell activation in vitro by inhibition of FGF, VEGF and PDGF signaling. *PLoS One* **9**, e92273, doi:10.1371/journal.pone.0092273 (2014).

118 Kyritsi, K. *et al.* Downregulation of p16 Decreases Biliary Damage and Liver Fibrosis in the Mdr2(/) Mouse Model of Primary Sclerosing Cholangitis. *Gene Expr* **20**, 89-103, doi:10.3727/105221620x15889714507961 (2020).

119 Li, J.-T., Liao, Z.-X., Ping, J., Xu, D. & Wang, H. Molecular mechanism of hepatic stellate cell activation and antifibrotic therapeutic strategies. *Journal of Gastroenterology* **43**, 419-428, doi:10.1007/s00535-008-2180-y (2008).

120 Antoine, M. *et al.* Expression and function of fibroblast growth factor (FGF) 9 in hepatic stellate cells and its role in toxic liver injury. *Biochem Biophys Res Commun* **361**, 335-341, doi:10.1016/j.bbrc.2007.06.189 (2007).

121 Tabibian, J. H., O'Hara, S. P., Splinter, P. L., Trussoni, C. E. & LaRusso, N. F. Cholangiocyte senescence by way of N-ras activation is a characteristic of primary sclerosing cholangitis. *Hepatology (Baltimore, Md.)* **59**, 2263-2275, doi:10.1002/hep.26993 (2014).

122 Yang, F. *et al.* Crosstalk between hepatic stellate cells and surrounding cells in hepatic fibrosis. *International Immunopharmacology* **99**, 108051, doi:https://doi.org/10.1016/j.intimp.2021.108051 (2021).

123 Ferreira Gonzalez, S. *et al.* Paracrine cellular senescence exacerbates biliary injury and impairs regeneration. *Nature Communications* **9**, doi:10.1038/s41467-018-03299-5 (2018).

124 Liang, G. *et al.* Fibroblast growth factor 1 ameliorates diabetic nephropathy by an anti-inflammatory mechanism. *Kidney International* **93**, 95-109, doi:https://doi.org/10.1016/j.kint.2017.05.013 (2018).

125 Zhao, L. *et al.* Fibroblast growth factor 1 ameliorates adipose tissue inflammation and systemic insulin resistance via enhancing adipocyte mTORC2/Rictor signal. *J Cell Mol Med* **24**, 12813-12825, doi:10.1111/jcmm.15872 (2020).

126 Wang, C. *et al.* Disruption of FGF Signaling Ameliorates Inflammatory Response in Hepatic Stellate Cells. *Front Cell Dev Biol* **8**, 601, doi:10.3389/fcell.2020.00601 (2020).

127 Khatri, P., Sirota, M. & Butte, A. J. Ten years of pathway analysis: current approaches and outstanding challenges. *PLoS Comput Biol* **8**, e1002375-e1002375, doi:10.1371/journal.pcbi.1002375 (2012).

128 Agarwal, V., Bell, G. W., Nam, J. W. & Bartel, D. P. Predicting effective microRNA target sites in mammalian mRNAs. *Elife* **4**, doi:10.7554/eLife.05005 (2015).

129 Wu, G. *et al.* Hepatitis B virus X protein downregulates expression of the miR-16 family in malignant hepatocytes in vitro. *Br J Cancer* **105**, 146-153, doi:10.1038/bjc.2011.190 (2011).

130 Li, L. *et al.* Human bile contains microRNA-laden extracellular vesicles that can be used for cholangiocarcinoma diagnosis. *Hepatology* **60**, 896-907, doi:10.1002/hep.27050 (2014).

131 Kim, K. M. *et al.* Gα(12) overexpression induced by miR-16 dysregulation contributes to liver fibrosis by promoting autophagy in hepatic stellate cells. *J Hepatol* **68**, 493-504, doi:10.1016/j.jhep.2017.10.011 (2018).

132 Zhu, B. *et al.* Increased miR-16 expression induced by hepatitis C virus infection promotes liver fibrosis through downregulation of hepatocyte growth factor and Smad7. *Archives of Virology* **160**, 2043-2050, doi:10.1007/s00705-015-2474-3 (2015).

133 He, Q. *et al.* miR-16 targets fibroblast growth factor 2 to inhibit NPC cell proliferation and invasion via PI3K/AKT and MAPK signaling pathways. *Oncotarget* **7**, 3047-3058, doi:10.18632/oncotarget.6504 (2016).

134 Pan, Q. *et al.* miR-16 integrates signal pathways in myofibroblasts: determinant of cell fate necessary for fibrosis resolution. *Cell Death Dis* **11**, 639, doi:10.1038/s41419-020-02832-z (2020).

135 Andriani, F. *et al.* MiR-16 regulates the pro-tumorigenic potential of lung fibroblasts through the inhibition of HGF production in an FGFR-1- and MEK1-dependent manner. *Journal of Hematology & Oncology* **11**, 45, doi:10.1186/s13045-018-0594-4 (2018).

136 Chamorro-Jorganes, A. *et al.* MicroRNA-16 and MicroRNA-424 Regulate Cell-Autonomous Angiogenic Functions in Endothelial Cells via Targeting Vascular Endothelial Growth Factor Receptor-2 and Fibroblast Growth Factor Receptor-1. *Arteriosclerosis, Thrombosis, and Vascular Biology* **31**, 2595-2606, doi:10.1161/ATVBAHA.111.236521 (2011).

137 Schelch, K. *et al.* A link between the fibroblast growth factor axis and the miR-16 family reveals potential new treatment combinations in mesothelioma. *Molecular oncology* **12**, 58-73, doi:10.1002/1878-0261.12150 (2018).